Computational Investigation of Phenyl-Substituted Polythiophenes

Taye Beyene Demisse

Department of Chemistry, Addis Ababa University
School of Graduate Studies
Addis Ababa, Ethiopia

June 2007

Computational Investigation of Conducting Polythiophenes and Substituted Polythiophenes

By

Taye Beyene Demisse

A Thesis Submitted to the
School of Graduate Studies of Addis Ababa University
In Partial Fulfillment of the Requirements for the Degree Of
Masters of Science in Chemistry

Addis Ababa University

July 2007

Declaration

This project is my original work, has not been presented for a degree in this and other University and that all resources and materials used for this project have been duly acknowledged.

Name: Taye Beyene Demisse
Signature: ------------------------

The project has been submitted for examination with our approval as University advisors.

	Name	Status	Singanture
1.	Dr. Ahmed Mustefa	As. Profesor	----------------------
2.	Dr. Shimelis Admasse	As. Profesor	-----------------------

Place and date of submission:
School of Graduate Studies
Addis Ababa University.
June 2007.

Acknowledgements

I am greatly indebted to my project advisors Dr. Ahmed Mustefa and Dr. Shimelis Admassie for their guidance and encouragement while I carry out this project work. I have no enough words to express their help during my study and this project work. Thank you once more.

I thank Dr. Mesfin Redi for his comment and moral support while I was doing this project work. Dr. Wendimagegn Mammo's help in providing necessary materials is also great for me. I also appreciate Dr. Teketel Yohannes for the materials that I got from him. Thank you very much all. I also greatly thank all my instructors and members of the department of chemistry of the Addis Ababa University.

I have benefited from the pray of my father Ato Beyene Demisse to God, and from the continuous support and encouragement of my sisters, brothers, family members and friends. Special thanks to Roza Mitiku, Tesfaye Alemayehu, Wubhareg Belay, Shewaye Wube, and Nigist Tesfaye. Thank you all.

Finally, I would like to express my sincere gratitude to the support and encouragement I got from my beloved wife W/o Tigist Wubshet. You showed great endurance in taking care of our son, Yohannes, and me. Waw, I have great appreciation to my son Yohannes Taye for his endurance and patience while I was apart from him. May God give you His rewards for your sacrifices!

"አመንበት አየነውም::"

Taye Beyene Demisse

Contents

Chapter One

Chapter Two

Chapter Three

Chapter Four

Chapter Five

List of Figures

List of Tables

List of Schemes

Abstract

Thiophene oligomers up to eight thiophene units and 3-(2,5-dialkoxyphenyl) thiophenes have been investigated using HF/STO-3G, DFT/STO-3G, DFT/3-21G*, and DFT/6-31G* computational levels. The structures are optimized to calculate the thermodynamic properties, UV-Vis absorption wavelength, and band gap of the oligomers. Increase in the number of thiophene rings increases the stability of both the doped and undoped states. The band gap decreases with increases in the number of thiophene rings. Up on oxidation, the band gap became further narrower compared with the neutral forms. Introducing dialkoxy phenyl-substituent at the 3-position of thiophene enhanced the stability and band gap of the oligomers. Longer alkoxy chains on the phenyl ring made the oligomers to be more stable and to have narrower band gap.

Key words: Thiophenes, density functional theory, band gap, excitation energy, and thermodynamic properties.

Chapter One

1.1 Project Description

Conjugated polymers have gained much interest due to their special electronic and optical properties [1-3]. Polymers are widely studied for different application purposes, for example in light emitting diodes, electrochromic materials, and solar cells [1-8]. In this project, we studied the electronic properties and thermodynamic properties of thiophenes, and three recently designed polymers, namely 3-(2,5-dibutyloxyphenyl) thiophene (DBOPT), 3-(2,5-diheptyloxyphenyl) thiophene (DHOPT), and 3-(2,5-dioctyloxyphenyl) thiophene (DOOPT). Focus is given on determining molecular geometry, electronic properties, and thermodynamic properties of the mentioned compounds since the major aim of this work is to determine the stability and electronic properties of the compounds and identifying stable compounds that are better for the application of the compounds in polymer materials. The calculated results are compared with experimental results reported, and based on such a comparison we suggested stable molecules and we extrapolated the results to the polymers. Both density functional theory and Hartree-Fock methods are used for the calculations on Gaussian 03W. STO-3G basis set is used in Hartree-Fock theory and STO-3G, 3-21G*, and 6-31G* basis sets are used in density functional theory calculations.

1.2 Project Outline

Chapter two gives a brief introduction to Computational Chemistry together with a more specific description of the theories used in the calculations. Chapter three introduces background of conjugated polymers. Chapter four contains the methodologies and compounds investigated in the project work. The results of the calculations are then presented and discussed in Chapter five, and lastly conclusions and possible recommendations are presented.

Chapter Two

Computational Chemistry

2.1 Introduction

The discovery processes of chemistry are more of descriptive and qualitative, but fundamentally it is a quantitative science [9]. The mathematical sciences provide the language for quantitative science, and this language is going in many directions as computational science. A timely opportunity now exists to strengthen and increase the beneficial impacts of chemistry by enhancing the interaction between chemistry and the mathematical sciences. This opportunity is used through computational chemistry [9,10].

Computational chemistry is an outgrowth of theoretical chemistry, which has sought to device and implement quantitative algorithms for organizing massive amounts of data from the laboratory, and for predicting the course and extent of chemical phenomena in situations that are difficult or even impossible to observe directly in the laboratory [9-12].

In quantum chemistry calculations different software are available, like Gaussian, GAMESS, DMOL and others. Among these Gaussian is the most widely used application software. Quantum Chemistry calculations are composed of different approximations and theories, among them semi-empirical, Hartree-Fock, and density functional theory are discussed in this study which are available in Gaussian 03W software.

2.2 Semi-empirical Methods

Semi-empirical methods are simplified versions of Hartree-Fock theory using empirical (derived from experimental data) corrections in order to improve performance. These methods are usually referred to through acronyms encoding some of the underlying theoretical assumptions. The most frequently used methods (MNDO, AM1, and PM3) are all based on the Neglect of Differential Diatomic Overlap (NDDO) integral approximation, while older methods use simpler integral schemes such as CNDO and INDO. All these approaches belong to the class of Zero Differential Overlap (ZDO) methods, in which all two-electron integrals involving two-center charge distributions are neglected. A number of additional approximations are made to speed up calculations and a number of parameterized corrections are made in order to correct for the approximate quantum mechanical model. For MNDO, AM1, and PM3 the parameterization is performed such that the calculated energies are expressed as heats of formations instead of total energies. The following are examples for semi-empirical methods [9-12]:

Table 1. Types of Semi empirical Methods

Acronym	Full name
CNDO	Complete Neglect of Differential Overlap
MNDO	Modified Neglect of Differential Overlap
AM1	Austin Model 1
PM3	Parametric Model Number 3

Semi-empirical methods are very useful in treating large molecules when a full Hartree-Fock calculation without approximations is too expensive. Semi-empirical calculations are much faster than *ab initio* calculation methods. However, the results may or may not be comparable with either experimental results or *ab initio* counterparts. The basis sets used in semi-empirical calculations are specially optimized minimal basis sets composed of Slater-type orbitals [11,12].

2.3 Hartree-Fock Methods

In order to describe the quantum mechanical behavior of all electrons in systems, it is strictly necessary to calculate the many-electron wave functions for the system using the time-independent Schrödinger equation [9,13]:

$$\frac{-\hbar^2}{2m}\frac{\partial^2}{\partial r^2}\Psi(r)+V\Psi(r)=E\Psi(r) \qquad [1.1]$$

where r represents displacement, m mass of the particle, $\hbar$ Plank's constant, Ψ the wave function, E energy, and V is the potential energy.

To solve the Schrödinger equation for all electrons in systems requires solving around 10^{23} simultaneous differential equations [13]. Such a calculation is very difficult and needs simplifying the methods and the problem itself. Hartree made such a simplification in 1928 through an iterative self-consistent field 'SCF' method. Hartree simplified the problem by making an assumption about the form of the many-electron wave functions; namely the product of a set of single-electron wave functions. In a uniform system these wave functions would take the form of simple plane waves. Having this assumption it was possible to proceed using the variational principle. According to the variational principle, if a given system is described by a set of unknown parameters the set of parameter values which correctly describes the ground state of the system is just that set of values which minimizes the total energy [9-13].

By using the variational method, Hartree found the Hamiltonian equation of the many-electron system and it was possible to treat each electron separately as a single-particle. The Hartree wave function is symmetric which stays precisely the same after interchange of two fermions, rather than antisymmetric. Therefore, the Hartree approach neglected the Pauli exclusion principle, which states that it is not possible for two fermions to exist at the same point in space with the same set of quantum numbers [9].

The Hartree product wave function is modified by Fock to overcome the problem encountered due to symmetric wave functions. Fock proposed the extension of Hartree's SCF procedure to Slater determinantal wave functions in order to meet the anti-symmetric nature of electrons. The Hartree approach is then improved and called Hartree-Fock approach in that the many-electron wavefunction is specially constructed out of single-electron wave functions in such a way to be antisymmetric. Just as with

Hartree product orbitals, the Hartree-Fock molecular orbitals can be individually determined as eigen-functions of a set of one-electron operators, but now the interaction of each electron with the static field of all of the other electrons includes exchange effects on the coulomb repulsion [10-13].

The wave function of Hartree-Fock approach is complicated than the Hartree product wave function, but it can be written in a compact way as a Slater determinant. Since electrons are fermions having a spin of ½, the total electronic wave function must be antisymmetric with respect to the interchange of any two-electron coordinates. The simplest antisymmetric function that is a combination of molecular orbitals is a determinant. The determinant considers the spin of all the electrons and the Pauli exclusion principle. The electrons can have a spin up (+1/2 or α) or spin down (-1/2 or β). The following is an example of a Slater determinant for a system of N-electrons [9-13]:

$$\Psi = \frac{1}{\sqrt{N!}} \begin{vmatrix} \Psi_1(1)\alpha(1) & \Psi 1(1)\beta(1) & \Psi 2(1)\alpha(1) & \Psi_2(1)\beta(1) \dots\dots\dots \Psi N(1)\alpha(1) & \Psi_N(1)\beta(1) \\ \Psi_1(2)\alpha(2) & \Psi 1(2)\beta(2) & \Psi_2(2)\alpha(2) & \Psi_2(2)\beta(2) \dots\dots\dots \Psi_N(2)\alpha(2) & \Psi N(2)\beta(2) \\ . & & . & . & \\ . & & . & . & \\ \Psi_1(N)\alpha(N) & \Psi_1(N)\beta(N) & \Psi_2(N)\alpha(N) & \Psi_2(N)\beta(N) \dots \Psi_N(N)\alpha(N) & \Psi_N(N)\beta(N) \end{vmatrix} \qquad [1.2]$$

where ψ is the electronic wave function , α and β spin of electrons and $\frac{1}{\sqrt{N!}}$ is a normalization factor.

2.4. Density Functional Theory

Density functional theory (DFT) is a quantum mechanical method used in physics and chemistry to investigate the electronic structure of many-electron systems, in particular molecules based up on a strategy of modeling electron correlation via general functionals of the electron density [10]. DFT is among the most popular and versatile methods available in computational physics and computational chemistry [11,12].

The predecessor to density functional theory was the Thomas-Fermi model, developed by Thomas and Fermi in 1927. They calculated the energy of an atom by representing its kinetic energy as a functional of the electron density, combining this with the classical expressions for the nuclear-electron and electron-electron interactions, which can both also be represented in terms of the electron density [9-13].

In DFT the main focus is not on the N-electron wave function $\Psi\left(\bar{x}_1,\bar{x}_2,.....\bar{x}_N\right)$ and the associated Schrödinger equation, but instead on the much simpler electron density $\rho\left(\bar{r}\right)$. The electron density is the number of electrons per unit volume for a given state. It is dependent only on 3 coordinates independently of the number of electrons of the system. Thus we have that:

$$N=\int \rho\left(\bar{r}\right)d\bar{r} \qquad [1.3]$$

The fundamental concept of DFT rely on the ground state energy and all other ground state electronic properties are uniquely determined by the electron density. Furthermore, the exact ground state of the system corresponds to the electronic density for minimal total energy. The total energy functional can be written as [9]:

$$\begin{aligned} E[\rho] &= T[\rho]+V_{ne}[\rho]+V_{ee}[\rho] \\ &= \int \rho\left(\bar{r}\right)V\left(\bar{r}\right)d\bar{r} + F[\rho] \end{aligned} \qquad [1.4]$$

where

$$F[\rho]=T[\rho]+V_{ee}[\rho]$$

$$V_{ee}[\rho] = J[\rho] + non-classical\,term$$

$$V\left(\bar{r}\right) = \sum_A \frac{Z_A}{\left|R_A-\bar{r}\right|}$$

$$J[\rho] = \frac{1}{2}\iint \frac{\rho\left(\bar{r}\right)\rho\left(\bar{r}'\right)}{\left|\bar{r}-\bar{r}'\right|}d\bar{r}d\bar{r}'$$

here $T[\rho]$ is the total kinetic energy, $V_{ne}[\rho]$ represents the electron - nuclei attraction, and $V_{ee}[\rho]$ represents the electron-electron interaction. $V\left(\bar{r}\right)$ is the external potential felt by an electron due to the nuclei. The term $J[\rho]$ is the classical columbic electron repulsion term.

Although density functional theory has its conceptual roots in the Thomas - Fermi model, DFT was not put on a firm theoretical footing until the Hohenberg-Kohn theorems (after Walter Kohn) (HK). The so-called Kohn-Sham equation is similar in form to the time-independent Schrödinger equation, except that the potential experienced by the electrons is formally expressed as a functional of the electron density and it is effectively a single-particle equation. The first of these demonstrates the existence of a one-to-one mapping between the ground state electron density and the ground state wavefunction of a many-particle system. Further, the second HK theorem proves that the ground state density minimizes the total electronic energy of the system. The original HK theorems held only for the ground state in the absence of magnetic field. The first Hohenberg-Kohn theorem is only an existence theorem, stating that the mapping exists, but does not provide any such exact mapping. It is in these mappings that approximations are made [9].

Traditional methods in electronic structure theory, in particular Hartree-Fock theory and its descendants, are based on the complicated many-electron wavefunction. The main objective of density functional theory is to replace the many-body electronic wavefunction with the electronic density as the basic quantity. The many-electron wavefunction is dependent on $3N$ variables, three spatial variables for each of the N electrons, whereas the density is only a function of three variables and is a simpler quantity to deal with both conceptually and practically [9].

The most common implementation of density functional theory is through the Kohn-Sham method. Within the framework of Kohn-Sham DFT, the interactable many-body problem of interacting electrons in a static external potential is reduced to a tractable problem of non-interacting electrons moving in an effective potential. The effective potential includes the external potential and the effects of the Coulomb interactions between the electrons, for example the exchange and correlation interactions. Modeling the latter two interactions becomes the difficulty within KS DFT. The simplest approximation is the local-density approximation (LDA), which is based upon exact exchange energy for a uniform electron gas, which can be obtained from the Thomas-Fermi model [11,12].

In many-body electronic structure calculations, the nuclei of the treated molecules or clusters are seen as fixed (the Born-Oppenheimer approximation), generating a static external potential V in which the electrons are moving. A stationary electronic state is then described by a wave function $\Psi\left(\vec{r_1},...,\vec{r_N}\right)$ fulfilling the many-electron Schrödinger equation [9-13]:

$$\hat{H}\Psi = [T+V+U]\Psi = \left[\sum_i^N -\frac{\hbar^2}{2m}\nabla^2{}_i + \sum_i^N V\left(\vec{r_i}\right) + \sum_{i>j} U\left(\vec{r_i},\vec{r_j}\right)\right]\Psi = E\Psi \qquad [1.5]$$

where $\hat{H}$ is the electronic molecular Hamiltonian, N is the number of electrons and U is the electron-electron interaction energy. The operators T and U are so-called universal operators as they are the same for any system, while V is system dependent or non-universal. The actual difference between a single-particle problem and the much more complicated many-particle problem just arises from the interaction term U. There are many sophisticated methods for solving the many-body Schrödinger equation based on the expansion of the wave function in Slater determinants, while the simplest one is the Hartree-Fock method. However, the problem with these methods is the huge computational effort, which makes it virtually impossible to apply them efficiently to larger, more complex systems. In DFT, the key variable is the particle density $n(\vec{r})$ which is given by:

$$n\left(\vec{r}\right) = N\int d^3r_2 \int d^3r_3 ... \int d^3r_N \Psi^*\left(\vec{r_1},\vec{r_2}..,\vec{r_N}\right)\Psi\left(\vec{r_1},\vec{r_2}..,\vec{r_N}\right) \qquad [1.6]$$

In the chemistry community, one popular functional is known as BLYP (from the name Becke for the exchange part and Lee, Yang and Parr for the correlation part) is the most widly used functional . Even more widely used is B3LYP which is a hybrid functional in which the exchange energy, in this case from Becke's exchange functional, is combined with the exact energy from Hartree-Fock theory. Along with the component exchange and correlation fucntionals, three parameters define the hybrid functional, specifying how much of the exact exchange is mixed in. The adjustable parameters in hybrid functionals are generally fitted to a set of molecules. The results obtained with these functionals are usually sufficiently accurate for most applications [11,12] .

2.5. Basis Sets in Computational Chemistry

A basis set is a set of functions used to create the molecular orbitals, which are expanded as a linear combination of such functions with the weights or coefficients to be determined. In modern computational chemistry, quantum chemical calculations are typically performed within a finite set of basis functions. When molecular calculations are performed, it is common to use a basis composed of a finite number of atomic orbitals, centered at each atomic nucleus within the molecule, for example linear combination of atomic orbitals. Initially, these atomic orbitals were typically Slater type orbitals, which corresponded to a set of functions, which decayed exponentially with distance from the nuclei. Later, it was realized that these Slater-type orbitals could in turn be approximated as linear combinations of Gaussian orbitals instead. Because it is easier to calculate overlap and other integrals with Gaussian basis functions, and this led to huge computational savings [11,12].

The basis functions employed by the *ab initio* Hartree-Fock and density functional methods for example are contracted Gaussian-type functions expressed by:

$$\chi_y = \sum_{w=1}^{b} d_{wy}\, g_w \qquad [1.7]$$

where the constants d_{wy} are called contraction coefficients, the g_w's are primitive Gaussians functions, and the values of b typically range from 1 to 7. The primitive Cartesian Gaussian function has the form:

$$g = N\, X^m\, Y^n\, Z^o\, e^{-\alpha r^2} \qquad [1.8]$$

The quantities m, n, and o are integers; X, Y, and Z are Cartesian coordinates; and α is the orbital exponent. When m + n + o = 0, then g is said to be a s-type Gaussian function; when m + n + o = 1, then g is a p-type Gaussian; and when m + n + o = 2, then g is a d-type Gaussian. By combining primitive Gaussian functions with different values of α contracted Gaussian functions that approximate the radial part of Slater-type orbitals (STOs) can be constructed. The advantage of the Gaussian function is that less computer time is required to evaluate the integrals. The values of the contraction coefficients d_{wy} and the orbital exponent α are obtained by fitting a contracted Gaussian function to an STO or by finding the contracted Gaussian functions that minimize the self-consistent-field energies of atoms. The basis sets used in Gaussian are classified in to minimal basis sets, split valency sets, multiple zeta basis sets and others.

2.5.1. Minimal Basis Sets

The minimal basis set is the minimum number of basis functions χ needed to describe the ground states of the component atoms in a molecule. For example, the minimal basis set for H_2O would be a 1s orbital for each hydrogen atom plus a 1s, 2s, $2p_x$, $2p_y$, and $2p_z$ orbital for the oxygen atom. Because the contraction coefficients d_{wy} and orbital exponent α are fixed, the size of a basis function on an atom cannot vary as the nature of the surrounding atoms changes. A common naming convention for minimal basis sets is STO-XG, where X is an integer. This X value represents the number of Gaussian primitive functions comprising a single basis function. In these basis sets, the same number of Gaussian primitives comprise core and valence orbitals. Minimal basis sets typically give rough results that are insufficient for research-quality publication, but are much cheaper than their larger counterparts. The following are examples of commonly used minimal basis sets: STO-2G, STO-3G, STO-6G [9,11,12].

2.5.2. Split-Valence Basis Sets

In a split-valence basis set the inner-shell atomic orbitals are represented by one basis function and the valence orbitals are represented by two or more basis functions. For example, the 3-21G basis set has one contracted Gaussian function that is a linear combination of three primitive Gaussian functions for each inner-shell atomic orbital and two basis functions, one contracted Gaussian function that is a linear combination of two primitive Gaussians and one primitive Gaussian function, for each valence orbital. To allow for the displacement of charge density away from the nuclei and toward the bonding regions, orbitals for which the l quantum number is greater than maximum value of the valence orbitals in the ground state atom are added to the basis set. The 6-31G* basis set represents each inner-shell orbital with one contracted Gaussian function, that is a linear combination of six primitive Gaussian functions and each valence orbital with two basis functions, one contracted Gaussian function that is a linear combination of three primitive Gaussians and one primitive Gaussian function. In addition, six d-type Gaussian functions for each non-hydrogen atom in the second or third period are included in the basis set.

Basis sets like 6-31G* are said to be polarized basis sets of the split valence basis sets. The notation for these split-valence basis sets is typically X-YZg. In this case, X represents the number primitive Gaussians comprising each core atomic orbital basis function. The Y and Z indicate that the valence orbitals are composed of two basis functions each, the first one composed of a linear combination of Y primitive Gaussian functions, the other composed of a linear combination of Z primitive Gaussian functions. In this case, the presence of two numbers after the hyphens implies that this basis set is a split-valence double-zeta basis set. The following are examples of commonly used split-valence basis sets: 3-21g, 3-21g* (Polarized), 3-21+g (Diffuse functions), 3-21+g* (With polarization and diffuse functions), 6-31g, and etc [9,11,12].

2.5.3 Multiple Zeta Basis Sets

Basis sets in which there are multiple basis functions corresponding to each atomic orbital, including both valence orbitals and core orbitals or just the valence orbitals, are called double, triple, or quadruple-zeta basis sets. Here is a list of commonly used multiple zeta basis sets: cc-pVDZ (Double-zeta), cc-pVTZ (Triple-zeta), cc-pVQZ (Quadruple-zeta), cc-pV5Z (Quintuple-zeta), etc. The 'cc-p' at the beginning of some of the above basis sets stands for 'correlation consistent polarized' basis sets and the V stands for valence. They are double/triple/quadruple-zeta for the valence orbitals only and include successively larger shells of polarization functions (p, d, f, g, etc.) that can yield convergence of the electronic energy to the complete basis set limit [9,11,12].

2.6 Calculation of Thermodynamic Properties

The equations used for computing thermo-chemical data in Gaussian 03W are equivalent to the equations in standard textbooks like McQuarrie and Levin on thermodynamics [9,13]. The thermodynamic properties are directly obtained from the frequency calculation that proceeds after optimization. Once the frequency calculation is carried out the thermodynamic properties like Gibbs free energy, enthalpy, entropy, contributing motions for the entropy, internal energy and etc of molecules can be extracted. The entropy, energy and heat capacity of the given molecules are contributed from translational, electronic, rotational, and vibrational motions. The starting point for the calculation of these motions is the partitions function q (V, T) for the corresponding components of the total partition function.

The partition function from any component can be used to determine the entropy contribution, S, from that component using the following relation:

$$S = Nk_B + Nk_B \ln\left(\frac{q(V,T)}{N}\right) + Nk_B T\left(\frac{\partial \ln q}{\partial T}\right)_V \qquad [1.9]$$

The $Nk_{B,}$ (k_B is the Boltzmann constant), value is represented by the universal gas constant R, and the equation will be reduced to:

$$
\begin{aligned}
S &= R + R\ln\left(q(V,T)\right) + RT\left(\frac{\partial \ln q}{\partial T}\right)_V \\
&= R\ln\left(q(V,T)e\right) + RT\left(\frac{\partial \ln q}{\partial T}\right)_V \\
&= R\left(\ln(q_t q_e q_r q_v e) + T\left(\frac{\partial \ln q}{\partial T}\right)_V\right)
\end{aligned}
\qquad [1.10]
$$

The internal thermal energy is also calculated from the partition function as given below:

$$q_r = \frac{\Pi^{1/2}}{\sigma_r}\left(\frac{T^{3/2}}{\left(\Theta_{r,x}\Theta_{r,y}\Theta_{r,z}\right)^{1/2}}\right) \qquad [1.11]$$

Once the energy is calculated, the heat capacity can also be calculated by using the following relation: $C_V = \left(\frac{\partial E}{\partial T}\right)_{N,V}$ [1.12]

The thermodynamic properties contributed by different motions play a great role in the calculations, which are discussed below.

2.6.1. Translational Contribution

In calculating thermodynamic properties contributed by translational motion of molecules, translational partition function plays the major role:

$$q_t = \left(\frac{2\Pi m k_B T}{h^2}\right)_V^{3/2} \qquad [1.13]$$

If the expression for q_t is derived with respect to temperature T, it gives

$$\left(\frac{\partial \ln q_t}{\partial T}\right)_V = \frac{3}{2T} \qquad [1.14]$$

This expression is used to calculate the internal energy and part of the calculation for entropy S. The value of volume, V, is approximated from the ideal gas equation, PV =

NRT = n / Nk$_B$T and V= k$_B$T / P and gives the equation for the partial partition function which is used to calculate the value of q$_t$ in Gaussian:

$$q_t = \left(\frac{2\Pi m k_B T}{h^2}\right)^{3/2} \frac{k_B T}{P} \qquad [1.15]$$

Once the value of transaltional partition function is obtained, the translational entropy and the internal energy can be calculated by using the following relations:

$$S_t = R\left(\ln\left(q_t e\right) + T\left(\frac{3}{2T}\right)\right) = R\left(\ln q_t + 1 + \frac{3}{2}\right) \qquad [1.16]$$

$$\begin{aligned} E_t &= N k_B T^2 \left(\frac{\partial \ln q}{\partial T}\right)_V \\ &= RT^2\left(\frac{3}{2T}\right) = \frac{3}{2}RT \end{aligned} \qquad [1.17]$$

And the transnational heat capacity at constant volume is calculated by using the following relation:

$$C_V = \frac{\partial E_t}{\partial T} = \frac{3}{2}R \qquad [1.18]$$

2.6.2. Rotational Contribution

The rotational partition function is of three types; rotational partititon function for monatomic particles, for linear diatomic particle, and for non-linear diatomic particles. The rotational partition function for monatomic particles is unity and the contribution for internal energy, entropy, and heat capacity are all zero since q$_r$ does not depend on temperature and no rotation takes place. For linear diatomic molecules, the rotational partition function is as follows:

$$q_r = \frac{1}{\sigma_r}\left(\frac{T}{\Theta_r}\right) \qquad [1.19]$$

Where $\Theta_r = h^2 / 8\Pi^2 I k_B$, I is the moment of inertia.

The rotational contribution to entropy is calculated using the following relation:

$$S_r = R\left(ln(q_r) + T\left(\frac{\partial ln q_r}{\partial T}\right)_V \right) \\ = R(ln q_r + 1) \qquad [1.20]$$

The internal energy is also given by:

$$E_r = RT^2\left(\frac{\partial \ln q_r}{\partial T}\right)_V = RT^2\left(\frac{1}{T}\right) = RT \qquad [1.21]$$

The following relation gives the contribution to the heat capacity at constant volume:

$$C_r = \left(\frac{\partial E_r}{\partial T}\right)_V = R \qquad [1.22]$$

The rotational contribution for the thermodynamic properties for a nonlinear molecule is dependent on the following rotational partition function:

$$q_r = \frac{\Pi^{1/2}}{\sigma r}\left(\frac{T^{3/2}}{\left(\Theta_{r,x}\Theta_{r,y}\Theta_{r,z}\right)^{1/2}}\right) \qquad [1.23]$$

From the above equations the differential part is given as,

$$\left(\frac{\partial ln q}{\partial T}\right)_V = \frac{3}{2T} \qquad [1.24]$$

Then the entropy due to rotational motion is given as:

$$S_r = R\left(\ln(q_r) + T\left(\frac{\partial \ln q_r}{\partial T}\right)_V \right) = R\left(\ln q_r + \frac{3}{2}\right) \qquad [1.25]$$

And the internal energy and the heat capacity for nonlinear molecules are given as follows:

$$E_r = RT^2\left(\frac{\partial \ln q_r}{\partial T}\right)_V = RT^2\left(\frac{3}{2T}\right) = \frac{3}{2}RT \quad \text{and,} \qquad [1.26]$$

$$C_r = \left(\frac{\partial E_r}{\partial T}\right)_V = \frac{3}{2}R \qquad [1.27]$$

2.6.3 Vibrational Contribution

For a molecule there are different vibrational modes, 3n-6 for nonlinear molecules and 3n-5 for linear molecules where n is the number of atoms. The characteristic temperature for vibrational motion is expressed as: $\Theta_{v,k} = hvk / k_B$ [1.28]

Then the vibrational partition function is given by the following equation:

$$q_{v,k} = \frac{e^{-\Theta_{v,k}/2T}}{1-e^{-\Theta_{v,k}/T}} \qquad [1.29]$$

And the overall vibrational partition function for the different vibrational modes is given by: $q_v = \prod_k \frac{e^{-\Theta_{v,k}/2T}}{1-e^{-\Theta_{v,k}/T}}$ [1.30]

If the vibrational energy level is assumed to be the zero of energy, then the overall partition function is given by:

$$q_v = \prod_k \frac{1}{1-e^{-\Theta_{v,k}/T}} \qquad [1.31]$$

In Gaussian the thermodynamic quantities are calculated by assuming the zero point of energy. Using this partition function Gaussian calculates the entropy, heat capacity and other thermodynamic properties. The total entropy contribution from the vibrational partition function is given by:

$$\begin{aligned} S_V &= R\left(\ln\left(q_v\right) + T\left(\frac{\partial \ln q}{\partial T}\right)_V \right) \\ &= R\left(\ln\left(q_v\right) + T\left(\sum_K \frac{\Theta_{V,K}}{2T^2} + \sum \frac{\left(\Theta_{V,K}/T^2\right)e^{-\Theta_{v,k}/T}}{1-e^{-\Theta_{v,k}/T}} \right)\right) \\ &= R\left(\sum_K \left(\frac{\Theta_{V,K}}{2T} + \ln\left(1-e^{-\Theta_{v,k}/T}\right)\right) + T\left(\sum_k \frac{\Theta_{V,K}}{2T^2} + \sum \frac{\left(\Theta_{v,k}/T^2\right)e^{-\Theta_{v,k}/T}}{1-e^{-\Theta_{v,k}/T}} \right)\right) \\ &= R\left(\sum_k \ln\left(1-e^{-\Theta_{v,k}/T}\right) + \left(\sum_k \frac{\left(\Theta_{v,k}/T\right)e^{-\Theta_{v,k}/T}}{1-e^{-\Theta_{v,k}/T}} \right)\right) \\ &= R\sum\left(\frac{\Theta_{V,K}/T}{e^{-\Theta_{v,k}/T}-1} - \ln\left(1-e^{-\Theta_{v,k}/T}\right)\right) \end{aligned} \qquad [1.32]$$

The internal energy and heat capacity are given by:

$$E_V = R\sum_k \Theta_{v,k}\left(\frac{1}{2}+\frac{1}{e^{\Theta_{v,k}/T}-1}\right) \qquad [1.33]$$

$$C_V = R\sum_k e^{\Theta_{v,k}/T}\left(\frac{\Theta_{v,k}/T}{e^{-\Theta_{v,k}/T}-1}\right)^2 \qquad [1.34]$$

2.6.4 Electronic Contribution

The electronic partition function is:

$$q_e = \varpi_0 e^{-\varepsilon_0/k_BT} + \varpi_1 e^{-\varepsilon_1/k_BT} + \varpi_2 e^{-\varepsilon_2/k_BT} + ... \qquad [1.35]$$

where ω is degeneracy of the energy level, and ε is energy for each level. In Gaussian the first electronic excitation energy is much greater than k_BT and therefore the first and higher excited states are assumed to be inaccessible at any temperature. Further the energy of the ground state is set zero. These assumptions simplify the electronic partition function to be:

$$q_e = \varpi_0 \qquad [1.36]$$

Which is simply the electronic spin multiplicity of the molecule. The entropy contributed by the electronic motion is calculated by using the following relation:

$$\begin{aligned} S_e &= R\left(ln(q_e)+T\left(\frac{\partial ln q_e}{\partial T}\right)_V\right) \\ &= R(ln q_e + 0) \end{aligned} \qquad [1.37]$$

The electronic heat capacity and the internal thermal energy due to electronic motion are zero, since there are no temperature dependent terms in the electronic partition function.

Chapter Three

Conducting Polymers

3.1 Introduction

Polymers are large molecules, or macromolecules, produced by the union of many monomers (10^2-10^6) or smaller repeating units. Conducting polymers have some similarities to conventional polymeric materials, but it is clearly the extensive main chain π-conjugation and its implicit stiffness with respect to chain bending and twisting that most influences the overall physical behavior. In other words conducting polymers contain high conjugation, which may not present in other polymers [1,14].

In the polymerization procedure, the first step is the formation of a positively charged species, which is a radical cation of the monomer. Then this radical cation reacts with another monomeric radical cation to form a dimmer. In the second step the dimmer loses one electron to form a radical cation of the dimmer, which reacts either with a monomeric radical cation to form a trimmer, or reacts with another dimmeric radical cation to form a tetrammer [1,3,14].

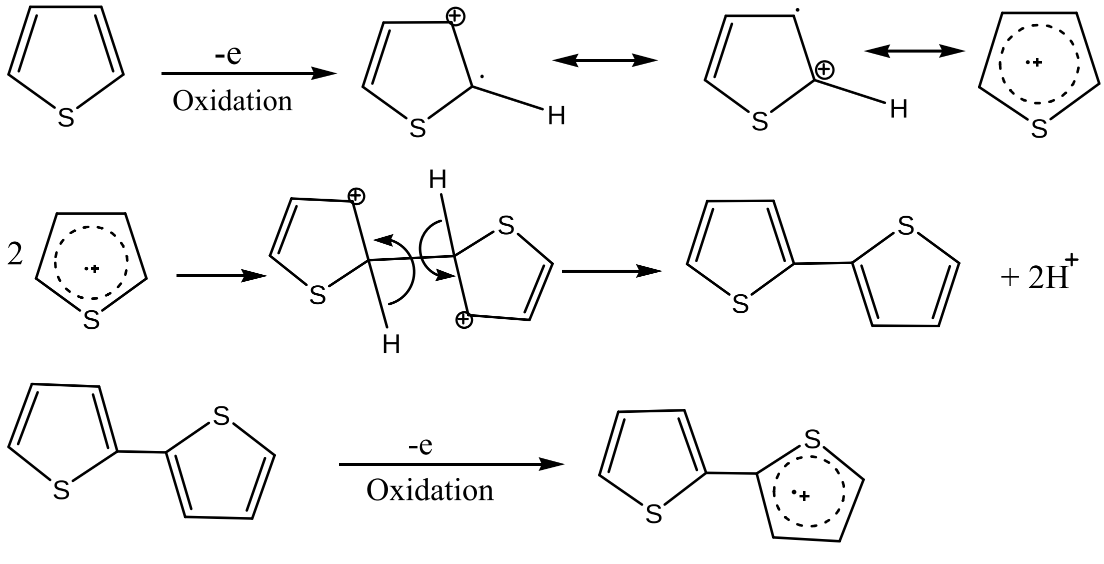

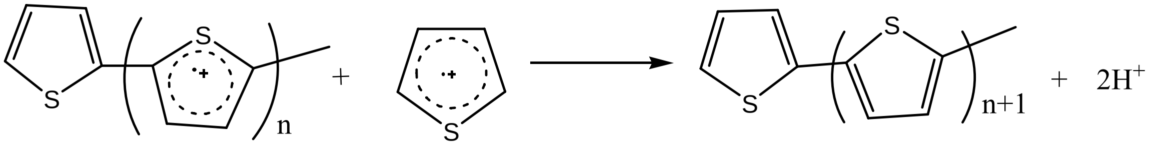

Scheme 1. The electropolymerization of thiophene molecules

When mono-substituted thiophenes are polymerized, three different couplings are possible: head-to-head (HH), head-to-tail (HT), or tail-to-tail (TT) [1,15,19,20].

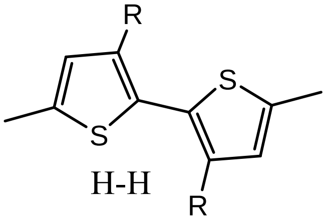

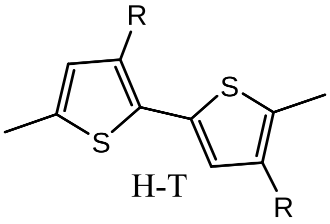

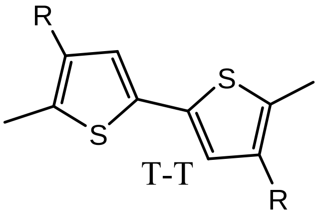

Some times asymmetric thiophene monomers are employed in polymerization to give structurally irregular polymers. The regiochemical couplings may result in the formation of head-to-head-tail-to-tail (HH-TT), head-to-tail-head-to-head (HT-HH), head-to-tail-head-to-tail (HT-HT) and tail-to-tail-head-to-tail (TT-HT) [3,19,20]. All the couplings show different optical properties at the same conditions [6].

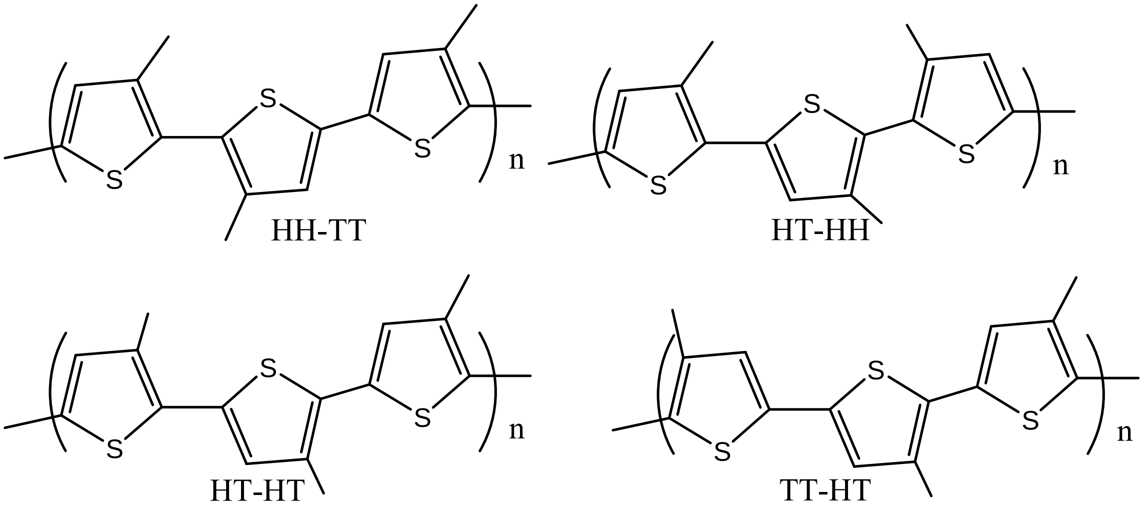

Scheme 2. Types of couplings in substituted polythiophenes

If all the thiophene rings are co-planar, the conjugation along the main chain is extended and the absorption occurs at a longer wavelength. Among the substituted thiophenes, the highest electron mobility, highest conductivity, and narrowest band gap is found in the perfect HT linked isomers. In addition, during the synthesis of polythiophenes the regularity of H-T coupling is high, for example in the Grignard type reaction about 93-96% coupling is H-T [1,19,20].

The property of most polymers, which distinguishes them from metals, is their inability to carry electricity. In fact, the insulating properties of polymers are a significant advantage for many applications of plastics. Electrical wires, for example, are protected from shorting by a coating of insulating polymer. In other words neutral conjugated polymers are insulators [1]. To make these polymers electrically conducting, one should introduce species, which are electron accepting (oxidizing agents) or electron donating (reducing agents) groups.

The oxidation and reduction reactions which induce high conductivity are termed, using the language of semiconductor physics, p-doping and n-doping, respectively. However, the process of doping in conducting polymers is different from that of semiconductors. In semiconductors doping involves replacing some of the atoms with atoms that have either more or less electrons, while in conducting polymers the dopant molecules never replace any of the atoms of the polymer; rather they simply act as associates that accept or donate electrons [1,14,15,16].

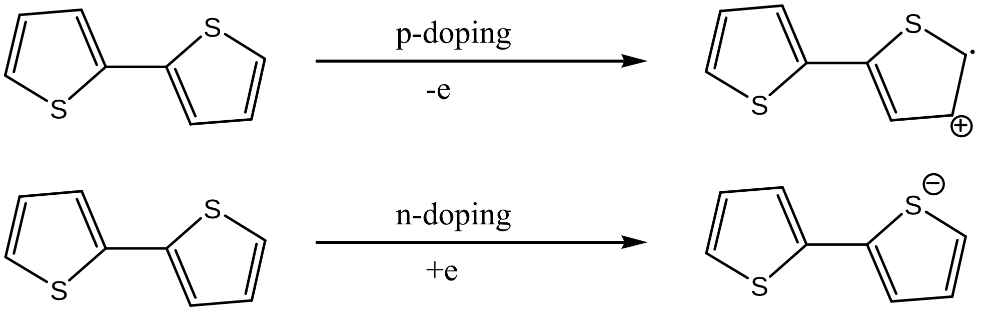

Scheme 3. Doping types in bithiophene molecule

Conducting polymers are initially insulators. Their metal like properties, that is their high conductivity and optical reflectivity, only become obvious after " doping". Even in the earliest stages of research on these materials, it was clear that these processes were not comparable with the classic doping of inorganic semiconductors. Rather, they correspond to oxidation in the case of p-doping or reduction in the case of n-doping. Suitable redox reagents are either chemical electron acceptors, or electron donors or the process may be electrochemically induced via an electrochemical cell. Because of the redox reaction the polymer chain is negatively charged in the case of reduction and positively charged in the case of oxidation. To maintain electro-neutrality, appropriate counter ions diffuse in to the polymer during charging and out of the polymers during discharging [14].

Conducting polymers formed from heteroatoms show different conformations. If the heteroatoms point in the same side the conformation is syn, while if the heteroatoms point in opposite directions the conformation is anti. For example this situation is observed in polythiophenes [14,16,17]:

Scheme 4. Anti and syn conformations in bithiophene molecule

NMR measurements indicate that the anti conformation is the most stable with a barrier for the conversion to the syn form of about 5 ± 2 Kcal/mol for polythiophenes. Electrons are delocalized along the conjugated backbones of conducting polymers, usually through overlap of π-orbitals, resulting in an extended π-system with a filled valence band [14,17,18].

By removing electrons from the π-system (p-doping), or adding electrons into the π-system (n-doping), a charged unit is formed. The charged unit moves up and down the polymer chain, and is responsible for the macroscopically observed conductivity of the polymer. Simultaneous oxidation of the conducting polymer and introduction of counter ions, p-doping, can be accomplished electrochemically or chemically. Reduction of the conducting polymer, n-doping, is much less common than p-doping.

An early study of electrochemical n-doping of polybithiophenes found that the n-doping levels are less than those of p-doping, the n-doping cycles were less efficient, the number of cycles required to reach maximum doping was higher, and the n-doping process appeared to be kinetically limited, possibly due to counter ion diffusion in the polymer [14,16].

When one electron is removed from neutral polymers a polaron is formed having only one charge. Removing a second electron from the polymer segment results not in two polarons, but in the bipolaron, which is predicted to be energetically more favored than the polaron. The reason is that the bipolaron is considerably greater than that for the polaron. The ionization energy required to remove a second electron decreases, or the electron affinity for taking up a second electron increases. For example the polaron and bipolaron formation of polythiophenes is shown below [14,16]:

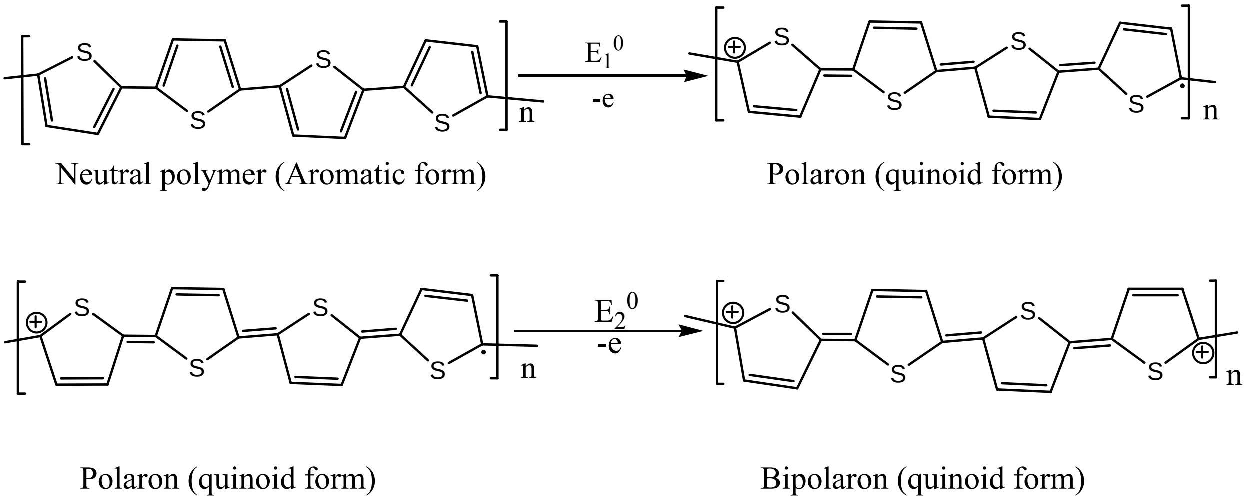

Scheme 5. Polaron and bipolaron formations in polythiophenes

The neutral conjugated polymer has full valence bands and empty conduction bands separated by a band gap. The generation of polarons and bipolarons creates two localized electronic levels, which are energetically separated in the energy gap. For polarons the discrete level within the gap is singly charged while for bipolarons it is all empty or all full depending on the doping type. Polarons have a spin of ½ whereas bipolarons are spineless. Their energy band picture is shown below [14]:

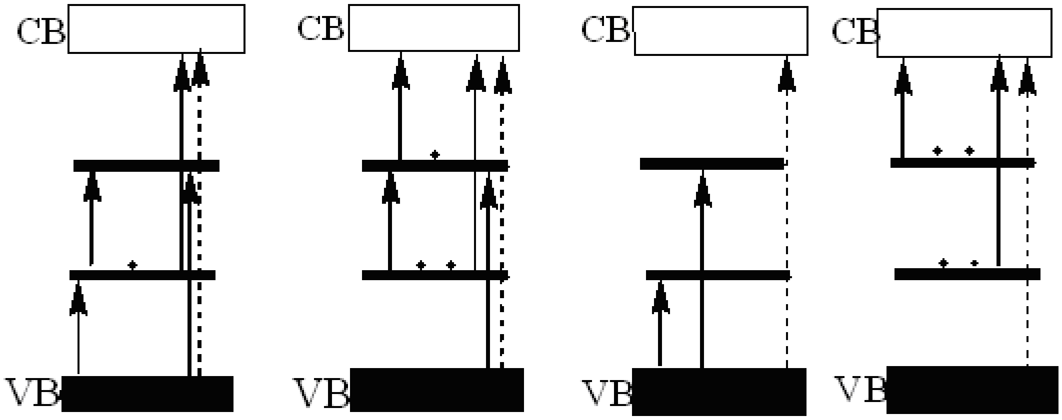

Charge +e Charge -e Charge +2e Charge -2e

Spin 1/2 Spin 1/2 Spin 0 Spin 0

Polarons Bipolarons

Fig.1 Energy band diagrams for polarons and bipolarons. The dark circles represent electrons, dashed arrows represent the possible allowed interband and the normal arrows represent the subgap transitions.

The doping process of conducting polymers can be represented by the following general scheme [14]:

For an oxidation process:

$$\text{Polymer} + X \longleftrightarrow (\text{Polymer})^{n+} + X^{n-}$$

and for a reduction process:

$$\text{Polymer} \quad + \quad \text{M} \quad \longleftrightarrow \quad (\text{Polymer})^{n-} \quad + \quad \text{M}^{n+}$$

Where X is the oxidizing agent and M is the reducing agent. X^{n-} and M^{n+} are the dopant counter anion and cation, respectively. The oxidizing agents can be I_2, Br_2, Cl_2, AsF_5, $FeCl_3$, and $NOPF_6$, and reducing agents like Li, Na, and K. P-type doping is more common than n-type doping because of the interference of oxygen in the n-doping process and also p-doping gives higher conductivity and better stability than n-doping. The electrical properties of conventional materials depend on how the bands are filled. When the bands are filled or empty, no conduction occurs. If the band gap is narrow, at room temperature thermal excitation of electrons from the valence band to the conduction band gives rise to conductivity. When the band gap is too wide, thermal excitation at room temperature is insufficient to excite electrons across the gap and become an insulator. The high conductivity of metals is due to a zero band gap.

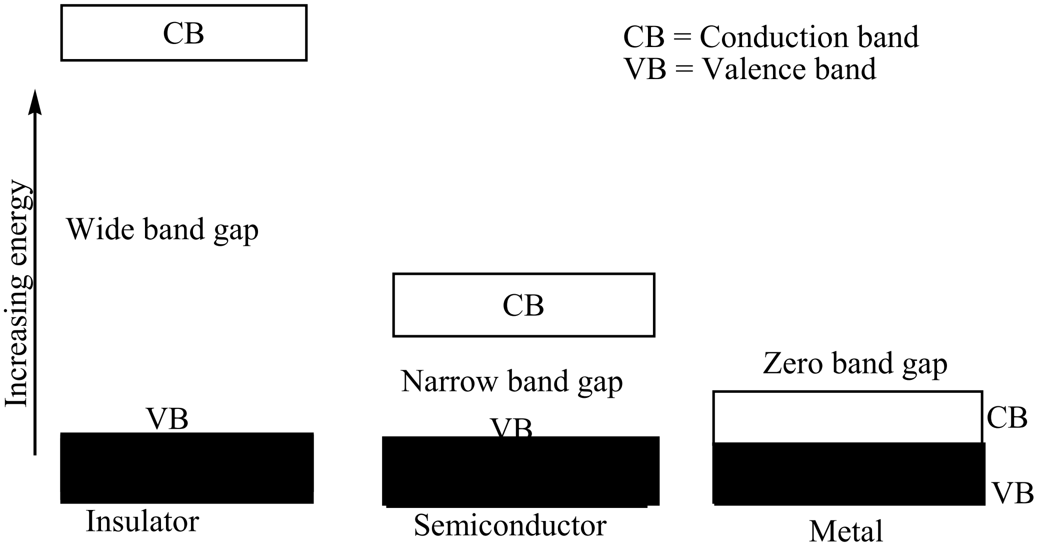

Fig.2 Energy band gap diagram for insulators, semiconductors, and metals.

In the case of conducting polymers when an electron is removed from the top of the valence band of a conjugated polymer a vacancy (hole or radical cation) is created that does not delocalize completely. Only partial delocalization occurs, extending over several monomeric units and causing them to deform structurally. The energy level associated with this radical cation represents a destabilized bonding orbital and thus has a higher energy than the energies in the valence band. In other words, its energy is in the band gap.

The stability of a doped conducting polymer is important for applications. Conducting polymers that have fewer, more regularly distributed side chains along the polymer backbone can be reduced by polymerizing bithiophenes or terthiophenes with only one side chain. Use of a phenyl ring between the flexible alkyl side chain and the polymer backbone increases the stability of the doped polymer. In other words when a phenyl ring is used as a spacer between the polymer back bone and the flexible side chain the polymeric back bone will become more rigid and gives more stable polymeric ion which can facilitate conditions for the delocalization of the charges. The stability therefore is dependent on the rigidity of the polymer main chain and the availability of space for the counter ion and the reactivity of the side groups [19].

3.2 Electrochromism in Polythiophenes

Electrochromism is defined as the electrochemical generation of color in accompaniment with an electron-transfer ('redox') reaction and is the phenomenon displayed by some chemical species of reversibly changing color when a burst of charge is applied on them [3]. Electrochromism is also broadly defined as a reversible optical change in a material induced by an external voltage, with many inorganic and organic species showing electrochromism throughout the electromagnetic spectrum. As the color change is persistent and energy need only be applied to effect a change, electrochromic materials are used, for example, to control the amount of light and heat allowed to pass through windows (smart windows), and has also been applied in the automobile industry to automatically tint rear-view mirrors in various lighting conditions [3,16].

Chemical or electrochemical oxidation of numerous resonance-stabilized aromatic molecules, such as pyrrole, thiophene, aniline, furan, azulene, indole, and others, produces electronically conducting polymers. In the oxidized state, conducting polymers are charge balanced, ‘doped’, with counter anions (‘p-doping’) and have a delocalized π-electron band structure. Reduction of ‘p-doped’ conducting polymers with concurrent counter anion exit (electrolyte cation incorporation) removes the electronic conjugation to give the ‘undoped’ (neutral) electrically insulating form. The energy gap (E_g, electronic band gap) between the highest occupied π-electron band (valence band) and the lowest unoccupied band (the conduction band) determines the intrinsic optical properties of these materials [3,16,20-23].

All conducting polymers are potentially electrochromic, redox switching giving rise to new optical absorption bands in accompaniment with simultaneous transport of electronic charge and counter ions in the polymer matrix. Oxidative p-doping shifts the optical absorption band towards the lower energy part of the spectrum. The color change or contrast between doped and undoped forms of the polymer depends on the magnitude of the band gap of the undoped polymer [3].

Thin films of conducting polymers with E_g greater than 3 eV (400nm) are colorless and transparent in the undoped form, while in the doped form they are generally absorbing in the visible region. Those with E_g equal to or less than 1.5 eV (800nm) are highly absorbing in the undoped form but, after doping the free carrier absorption is relatively weak in the visible region as it is transferred to the near infrared [20,24].

Polymers with intermediate gaps have distinct optical changes throughout the visible region and can be made to induce many color changes. From the electrochromic polymer materials, polythiophenes taken the main consideration due to their ease of chemical and electrochemical synthesis, environmental stability, and processability. A large number of substituted thiophenes have been synthesized and this has led to the study of numerous novel polythiophenes [20-27].

The spectro-electrochemical properties of thiophene polymers also attracted much attention due to the possibilities of their application in the optical industry. Besides their exceptional stability, thiophene derivatives can be easily synthesized at a low cost and provide reasonable contrast in multiple colors. These features make them good candidates for use in displays, mirrors, and smart windows. The reason for the spectacular development of these compounds are related to their good environmental stability, in both neutral and doped states [34-38], and to their structural versatility which has led to the synthesis of a large number of substituted derivatives as a way of improving and controlling the electrical and optical properties [20-26].

Substitution effects influence the position of the oxidation potentials of the polymers and the structure of the polymers plays a dominant role in determining the physical properties of conducting polymers. Although electron-donating substituents lower oxidation potentials just as they do in the monomers [36-42], the electron withdrawing substituents raise them [3, 27]. The chain length of the substituted alkyl or alkoxy groups have also an effect on the electrochemical properties of polymers derived from the 3-alkyl substituted polythiophenes.

Chapter Four

Objectives, Computational Methods, and Compounds

4.1 Objectives

The objectives of this research project are:

1. to optimize geometries and calculate thermodynamic properties of oligothiophenes and phenyl-Substituted-oligothiophenes,
2. to compare the results of this study with that of literature reports, and
3. to identify stable polymers which can be used in conducting polymer materials

4.2 Computational Methods

The structures of the reduced and oxidized (radical cation or polaron) forms of the compounds studied were optimized by Becke's three parameter hybrid functional for exchange combined with the correlation functional due to Lee, Yang, and Parr (B3LYP) [10, 11, 29] and Hartree-Fock methods at STO-3G, 3-21G*, and 6-31G* levels. The optimized structures of the oxidized forms were obtained by removing an electron from the optimized geometries of the reduced forms performing further optimizations. For the odd-ring number oligothiophenes C_{2v} symmetry [22] is used and for the even-ring numbers C_{2h} symmetry [22] is used through out the calculations. For the phenyl-substituted thiophenes C_1 symmetry is used.

Based on the optimized geometries the thermodynamic properties for all the compounds were calculated by HF methods using STO-3G basis set and B3LYP method using STO-3G, and 3-21G* basis sets. The changes in the thermodynamic properties were computed by subtracting the thermodynamic property of the reduced forms from the thermodynamic property of the oxidized forms. For all closed-shell calculations the restricted orbital arrangement and for all open-shell calculations the unrestricted arrangements were employed. The excitation energies and maximum absorption wavelengths of the reduced forms of the oligomers were calculated by time dependent density functional theory (TDDFT) method at 3-21G* and 6-31G* levels. The HOMO and LUMO energies were obtained from the energy calculations of both the neutral and oxidized forms of the compounds. All the calculations were performed at 298.15K and 1.00atm using Gaussian 03 program package [29].

4.3 Compounds Investigated

Polythiophenes, class of conjugated polymers, have been studied intensively for the application of light emitting diodes, solar cells, and electrochromic materials [3,4,14,21,23]. Introducing side chains on the polythiophene backbone makes the polymer soluble and processable [30-33,42-45]. In addition, side chains incorporated have a profound influence on the band gap and stability of the polymers [30]. In order to study the stability, band gap, and other electronic properties of polythiophenes and substituted polythiophenes, the calculation is started from simple thiophene units and continued to the polythiophene unit having eight monomer units. Next to the thiophene units, different compounds with substituents on the phenyl unit of the 3-phenylthiophenes are considered. The structures for all the compounds are given in scheme 6:

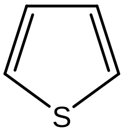

I. Thiophene

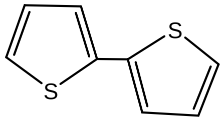

II. Dimmer of thiophene

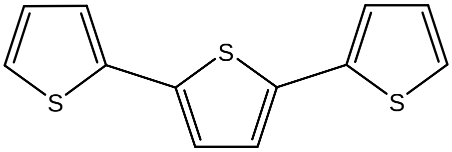

III. Trimmer of thiophene

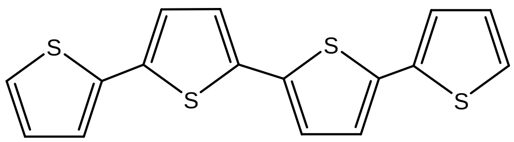

IV. Tetrammer of thiophene

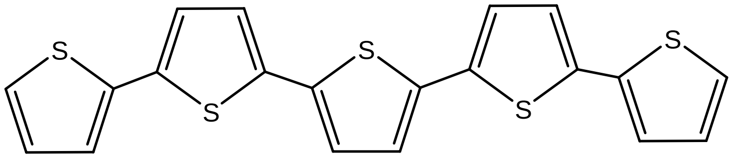

V. Pentammer of thiophene

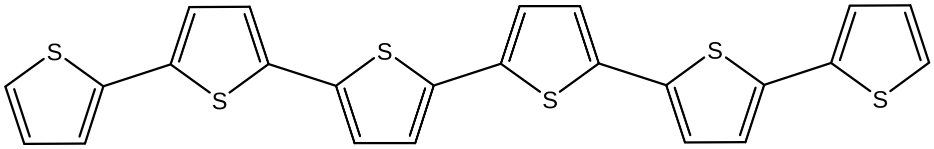

VI. Hexammer of thiophene

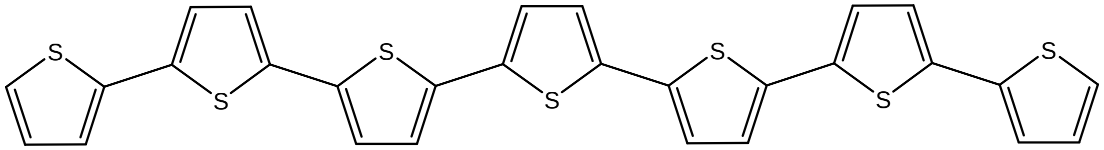

VII. Heptammer of thiophene

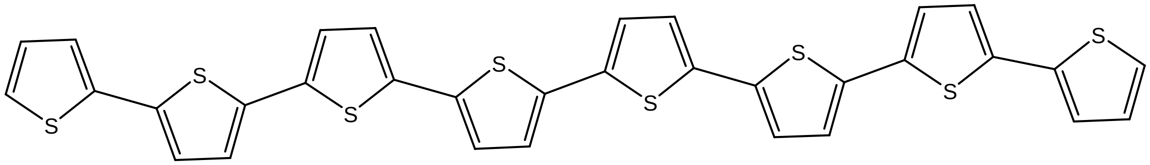

VIII. Octammer of thiophene

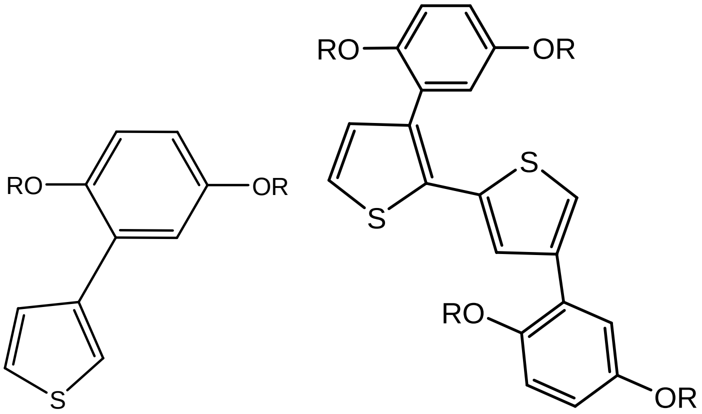

IX. **DBOPT**, [3-(2,5-dibutyloxyphenyl) thiophene], R = $-(CH_2)_3CH_3$

X. **DHOPT**, [3-(2,5-diheptyloxyphenyl) thiophene], R = $-(CH_2)_6CH_3$

XI. DOOPT, [3-(2,5-dioctyloxyphenyl) thiophene], R = $-(CH_2)_7CH_3$

Scheme 6. Structures of the investigated compounds

Chapter Five

Results and Discussion

5.1 Structural Parameters

To extract the structural parameters the numbering system for oligothiophenes given in scheme 6 is followed.

5.1.1 Thiophene oligomers

The thiophene oligomers are investigated starting from the thiophene unit up to the octammer of thiophene in which their structures are given in scheme 6. From the optimized structure of the compounds, bond lengths and bond angles are extracted and listed in tables2-18.

Table 2. Optimized bond length (in Å) of oligothiophenes in neutral (reduced) and polaronic (oxidized) states obtained at **B3LYP/ STO-3G** level.

Parameter	Number of thiophene rings							
	1		2		3		4	
	Red	Oxd	Red	Oxd	Red	Oxd	Red	Oxd
C_1C_2	1.3718	1.44741	1.3742	1.41211	1.37446	1.3979	1.3746	1.3907
C_2C_3	1.4519	1.39875	1.4432	1.40869	1.44259	1.41930	1.4424	1.4259
C_3C_4	1.3718	1.44741	1.3885	1.43643	1.38962	1.41971	1.3898	1.4104
C_4S_5	1.7527	1.75622	1.7707	1.78966	1.77131	1.78227	1.7714	1.7780
S_5C_1	1.7527	1.75622	1.7502	1.73248	1.74969	1.73587	1.7497	1.7390
C_4C_6	-	-	1.4732	1.42488	1.46985	1.43411	1.4693	1.4436
C_6C_7	-	-	1.3885	1.43643	1.39213	1.43590	1.3928	1.4274
C_7C_8	-	-	1.4432	1.40869	1.43281	1.39636	1.4318	1.4014
C_8C_9	-	-	1.3742	1.41211	1.39213	1.43590	1.3936	1.4287
C_6S_{10}	-	-	1.7707	1.78966	1.76828	1.77093	1.7681	1.7655
C_9S_{10}	-	-	1.7502	1.73248	1.76828	1.77093	1.7689	1.7751
C_9C_{11}	-	-	-	-	-	-	1.4665	1.4303

The calculated structural parameters are given in tables 2 and 3. From table 2 it is observed that up on the removal of an electron from the neutral compounds the bond lengths of the oligommers changed. Single bonds become shorter and double bonds become longer in the oxidized structures than the reduced (neutral) structures. Whereas the lengths of the double bonds in the oxidized state are longer than the length of double bonds in the neutral forms and the lengths of single bonds in the oxidized state are shorter than lengths of single bonds of the neutral forms. This shows that up on oxidation the single bonds show double bond character and the double bonds show single bond character and this implies the emerging of quinoid character of the oligommers.

Table 3. Optimized bond length (in Å) of oligothiophenes in neutral (reduced) and polaronic (oxidized) states obtained at **B3LYP/3-21G*** level.

Parameter	Number of thiophene rings							
	1		2		3		4	
	Red	Oxd	Red	Oxd	Red	Oxd	Red	Oxd
C_1C_2	1.3697	1.43107	1.3700	1.40046	1.37010	1.38909	1.3703	1.3835
C_2C_3	1.4349	1.38109	1.4272	1.39277	1.42722	1.40348	1.4266	1.4097
C_3C_4	1.3697	1.43107	1.3807	1.42044	1.38147	1.40647	1.3817	1.3987
C_4S_5	1.7355	1.73101	1.755	1.76917	1.75635	1.76423	1.7564	1.7608
S_5C_1	1.7355	1.73101	1.7348	1.71176	1.73423	1.71534	1.7342	1.7187
C_4C_6	-	-	1.4483	1.40056	1.44400	1.40933	1.4435	1.4183
C_6C_7	-	-	1.3807	1.42044	1.38171	1.41817	1.3825	1.4114
C_7C_8	-	-	1.4273	1.39277	1.41877	1.38235	1.4171	1.3873
C_8C_9	-	-	1.3700	1.40046	1.38171	1.41817	1.3835	1.4126
C_6S_{10}	-	-	1.755	1.76917	1.75531	1.75547	1.7553	1.7512
C_9S_{10}	-	-	1.7348	1.71176	1.75531	1.75547	1.7563	1.7601
C_9C_{11}	-	-	-	-	1.44400	1.40933	1.4435	1.4054
$C_{11}C_{12}$	-	-	-	-	1.38147	1.40647	1.3817	1.4126
$C_{12}C_{13}$	-	-	-	-	1.42722	1.40348	1.4266	1.3873
$C_{13}C_{14}$	-	-	-	-	1.37010	1.38909	1.3703	1.4114
$C_{11}S_{15}$	-	-	-	-	1.75635	1.76423	1.7564	1.7601

The inter-rings bonds are longer than normal double bonds but shorter than the single bonds. From these bond lengths it is also possible to confirm the emerging of a quinoidal-like distortions as a result of oxidation. For the longer oligommers the quinoidal character is situated in the innermost rings. This is observed from the change in bond lengths of C_1C_2 and $C_{16}C_{17}$ of octathiophene. From table 4 the bond length of C_1C_2 in the neutral form is 1.3704 Å while in the oxidized form it is 1.3756 Å, which shows a very small difference (0.0052 Å), but $C_{16}C_{17}$ in the neutral form is 1.3849 Å while in the oxidized form it is 1.404 Å, which shows larger change in bond length (0.019 Å) when compared with C_1C_2 of octathiophene.

Table 4. Optimized bond length (in Å) of oligothiophenes in neutral (reduced) and polaronic (oxidized) states obtained at **B3LYP/3-21G*** level.

Parameter	Number of thiophene rings							
	5		6		7		8	
	Red	Oxd	Red	Oxd	Red	Oxd	Red	Oxd
C_1C_2	1.3704	1.38019	1.3707	1.37808	1.37041	1.37664	1.3704	1.3756
C_2C_3	1.4265	1.41367	1.4262	1.41631	1.42666	1.41817	1.4266	1.4195
C_3C_4	1.3819	1.39426	1.3825	1.39137	1.38189	1.38944	1.3819	1.3882
C_4S_5	1.7563	1.75893	1.7555	1.75779	1.75610	1.75710	1.7560	1.7567
S_5C_1	1.7341	1.72130	1.7340	1.72327	1.73383	1.72478	1.7338	1.7259
C_4C_6	1.4433	1.42415	1.4434	1.42834	1.44334	1.43127	1.4434	1.4334
C_6C_7	1.3828	1.40569	1.3836	1.40135	1.38285	1.39813	1.3829	1.3957
C_7C_8	1.4168	1.39241	1.4159	1.39671	1.41681	1.40003	1.4168	1.4026
C_8C_9	1.3838	1.40658	1.3846	1.40189	1.38385	1.39843	1.3839	1.3959
C_6S_{10}	1.7551	1.75002	1.7545	1.74966	1.75488	1.74977	1.7548	1.7501
C_9S_{10}	1.7565	1.76048	1.7558	1.75983	1.75637	1.75914	1.7563	1.7585
C_9C_{11}	1.4391	1.40939	1.4388	1.41409	1.43895	1.41813	1.4389	1.4214
$C_{11}C_{12}$	1.3843	1.41124	1.3852	1.40799	1.38453	1.40473	1.3846	1.4019
$C_{12}C_{13}$	1.4158	1.38751	1.4147	1.39050	1.41550	1.39378	1.4154	1.3967
$C_{13}C_{14}$	1.3843	1.41124	1.3853	1.40774	1.38465	1.40412	1.3847	1.4010
$C_{11}S_{15}$	1.7564	1.75760	1.7557	1.75577	1.75613	1.75468	1.7562	1.7541
$C_{14}S_{15}$	1.7564	1.75760	1.7559	1.75914	1.75647	1.75926	1.7564	1.7589
$C_{14}C_{16}$	-	1.40939	1.4383	1.41026	1.43820	1.41321	1.4382	1.4164
$C_{16}C_{17}$	-	-	-	-	1.38481	1.40626	1.3849	1.4040
$C_{17}C_{18}$	-	-	-	-	1.41519	1.39188	1.4151	1.3942
$C_{19}S_{20}$	-	-	-	-	1.75641	1.75768	1.7564	1.7581
$C_{19}C_{21}$	-	-	-	-	-	1.41321	1.4380	1.4149

For a thiophene molecule the adjacent C-S bond lengths are identical in the reduced form, and this result is also observed for the oxidized form since they are in identical chemical environments. The extreme carbon-sulfur bonds of dimmers and above (C_5-S_1 for example) have decreased in its length whereas the carbon-sulfur bond that is adjacent to the next ring (S_1-C_2 for example) has increased from similar bonds of the oligomers.

Table 5. Optimized bond length (in Å) of oligothiophenes in neutral (reduced) and polaronic (oxidized) states obtained at **B3LYP/6-31G*** level.

Parameter	Number of thiophene rings							
	1		2		3		4	
	Red	Oxd	Red	Oxd	Red	Oxd	Red	Oxd
C_1C_2	1.3674	1.4238	1.3672	1.3957	1.3675	1.3851	1.3678	1.3799
C_2C_3	1.4298	1.3798	1.4235	1.3914	1.4231	1.4014	1.4225	1.4072
C_3C_4	1.3674	1.4238	1.3783	1.4161	1.3796	1.4031	1.3802	1.3957
C_4S_5	1.7356	1.7317	1.7353	1.7698	1.7355	1.7654	1.7359	1.7623
S_5C_1	1.7356	1.7317	1.7567	1.7152	1.7582	1.7183	1.7580	1.7214
C_4C_6	-	-	1.4508	1.4059	1.44678	1.4138	1.4461	1.4224
C_6C_7	-	-	1.3783	1.4161	1.37936	1.4137	1.3806	1.4073
C_7C_8	-	-	1.4235	1.3914	1.41583	1.3819	1.4140	1.3866
C_8C_9	-	-	1.3672	1.3957	1.37936	1.4137	1.3816	1.4086
C_6S_{10}	-	-	1.7567	1.7698	1.75748	1.7578	1.7575	1.7539
C_9S_{10}	-	-	1.7353	1.7152	1.75748	1.7578	1.7585	1.7623
C_9C_{11}	-	-	-	-	1.44678	1.4138	1.4421	1.4092
$C_{11}C_{12}$	-	-	-	-	1.37959	1.4031	1.3816	1.4086
$C_{12}C_{13}$	-	-	-	-	1.42306	1.4014	1.4140	1.3866
$C_{13}C_{14}$	-	-	-	-	1.36751	1.3851	1.3806	1.4073
$C_{11}S_{15}$	-	-	-	-	1.75816	1.7654	1.7585	1.7623
$C_{14}S_{15}$	-	-	-	-	1.73553	1.7183	1.7575	1.7539
$C_{14}C_{16}$	-	-	-	-	-	-	1.4461	1.4224

Table 6. Optimized bond length (in Å) of oligothiophenes in neutral (reduced) and polaronic (oxidized) states obtained at **B3LYP/6-31G*** level.

Parameter	Number of thiophene rings							
	5		6		7		8	
	Red	Oxd	Red	Oxd	Red	Oxd	Red	Oxd
C_1C_2	1.3677	1.3373	1.3677	1.3749	1.36765	1.37347	1.3677	1.3725
C_2C_3	1.4228	1.4111	1.4228	1.4133	1.42285	1.41503	1.4225	1.4163
C_3C_4	1.3799	1.3911	1.3799	1.3888	1.37993	1.38692	1.3802	1.3856
C_4S_5	1.7353	1.7610	1.7354	1.7594	1.73538	1.75890	1.7359	1.7585
S_5C_1	1.7583	1.7240	1.7583	1.7255	1.75822	1.72695	1.758	1.7281
C_4C_6	1.4460	1.4270	1.4460	1.4321	1.44594	1.43480	1.4459	1.4368
C_6C_7	1.3803	1.4019	1.3803	1.3979	1.38036	1.39481	1.3807	1.3925
C_7C_8	1.4143	1.3918	1.4145	1.3957	1.41433	1.39869	1.4138	1.4011
C_8C_9	1.3813	1.403	1.3814	1.3984	1.38138	1.39514	1.3817	1.3927
C_6S_{10}	1.7575	1.753	1.7574	1.7523	1.75747	1.75252	1.7575	1.7528
C_9S_{10}	1.7588	1.762	1.7589	1.7619	1.75888	1.76137	1.7588	1.7608
C_9C_{11}	1.4418	1.4128	1.4415	1.4178	1.44147	1.42168	1.4412	1.4248
$C_{11}C_{12}$	1.3818	1.4067	1.382	1.4044	1.38204	1.40127	1.3824	1.3986
$C_{12}C_{13}$	1.4135	1.3868	1.4132	1.3897	1.41316	1.39277	1.4126	1.3955
$C_{13}C_{14}$	1.3818	1.4067	1.3820	1.4042	1.38217	1.40071	1.3825	1.3978
$C_{11}S_{15}$	1.7587	1.7602	1.7588	1.7583	1.75868	1.75722	1.7587	1.7567
$C_{14}S_{15}$	1.7587	1.7602	1.7589	1.7614	1.75901	1.76163	1.7590	1.7614
$C_{14}C_{16}$	1.4418	1.4128	1.441	1.4139	1.44073	1.41673	1.4405	1.4198
$C_{16}C_{17}$	-	-	-	-	1.38232	1.40280	1.3827	1.4007
$C_{17}C_{18}$	-	-	-	-	1.41283	1.39087	1.4123	1.3931
$C_{19}S_{20}$	-	-	-	-	1.38232	1.40280	1.3828	1.7607
$C_{19}C_{21}$	-	-	-	-	1.75898	1.76016	1.7589	1.4183

The C-C and C-S bonds of the two adjacent rings of bithiophene are identical to one another since their lengths are identical, for example C_1-C_2 = C_8-C_9 = 1.40046 Å for the oxidized bithiophene, table 3 above. This condition is also observed for both of the corresponding thiophene rings of the other oligommers. It is clear from the tables 5 and 6 that as the number of rings increase the length of single and double bonds show very slight difference or become consistent. This implies that the theoretical investigation of longer oligommers can be considered as model for the investigation of the polymers.

The lengthening of double bonds and shortening of the single bonds is considered as a possible evidence for the formation of a quinoid structural arrangements at the oxidized states. Depending on this evidence the following scheme can explain the formation of quinoidal structures from the aromatic structures.

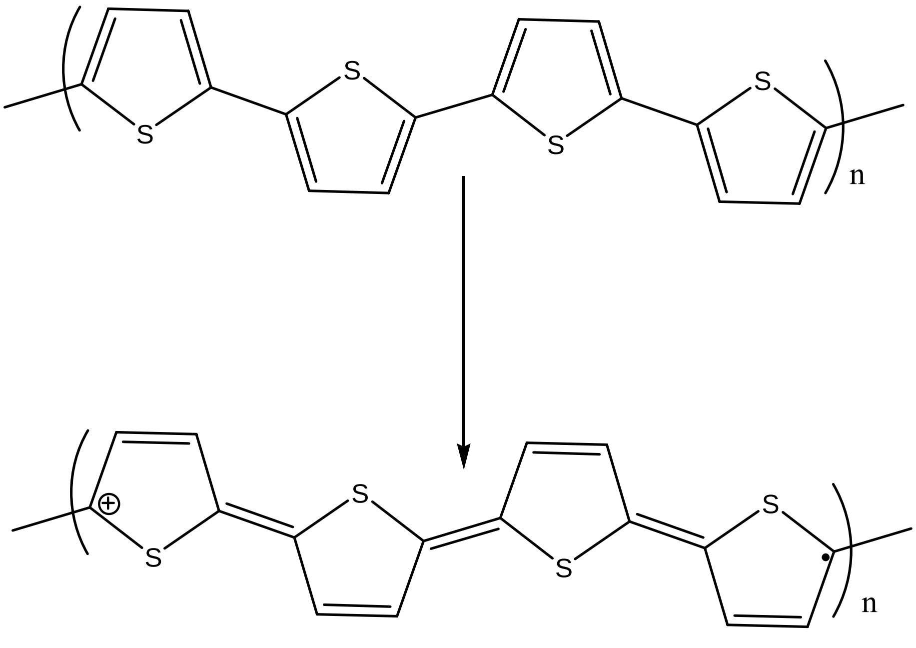

Scheme 7. Structure of aromatic and quinoid forms of the polythiophene

5.1.2 Comparison with Earlier Theoretical and Experimental Results

The structural parameters calculated in this work are listed with earlier theoretical and experimental results reported in literatures.

5.1.2.1 Thiophene

The bond lengths and bond angles of a thiophene unit obtained in this work are listed with reported experimental and theoretical results in table7.

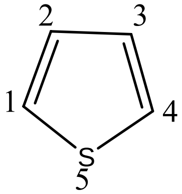

Table 7. Bond lengths and bond angles of neutral thiophene molecule

Parameter	This work (DFT/3-21G*)	This work (DFT/6-31G*)	Ref. 41 (Exp)[a]	Ref.18 (Exp)[b]	Ref.18 (cal) HF/6-31G*
C_1C_2	1.3697	1.3674	1.370	1.3696	1.3451
C_2C_3	1.4349	1.4298	1.423	1.4232	1.4369
C_3C_4	1.3697	1.3674	1.370	1.3696	1.3451
C_4S_5	1.7355	1.7356	1.714	1.714	1.7258
S_5C_1	1.7355	1.7356	1.714	1.714	1.7258
$C_1C_2C_3$	112.59166	112.73682	112.5	112.45	112.53
$C_2C_3C_4$	112.59166	112.73682	112.5	112.45	112.53
$C_3C_4S_5$	111.63533	111.50334	111.5	111.47	111.84
$C_4S_5C_1$	91.54603	91.51969	92.2	92.17	91.27
$S_5C_1C_2$	111.63533	111.50334	111.5	111.47	111.84

[a] =X-ray crystallography measurement, [b] = solid-state x-ray data

Considering C-C and C-S bond lengths, methods used in this work estimated a satisfactory result with the experimental but the theoretical result reported using HF/6-31G* are slightly different from the experimental results compared with our results. The bond angles calculated in this work and reported theoretical result are in close agreement with the experimental results except $C_3C_4S_5$ and $S_5C_1C_2$ which are over estimated in the reported HF/6-31G* method.

The structural parameters calculated in this work are in close agreement with the experimental results.

5.1.2.2 Bithiophene

For a bithiophene unit the experimental results obtained did not include the bond angles hence we compared only the bond lengths with both experimental and theoretical results. The following numbering system is followed for the extraction of the structural parameters of bithiophene.

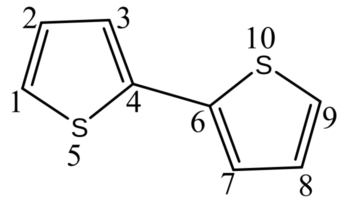

Table 8. Bond length of neutral bithiophene molecule

Parameter	This work (DFT/3-21G*)	This work (DFT/6-31G*)	[18] (exp)^b	[33] (exp)^c	[17] UB3-PW91/cc-pVDZ
C_1C_2	1.3700	1.3672	1.35	1.3444	1.33531
C_2C_3	1.4272	1.4235	1.413	1.4336	1.44789
C_3C_4	1.3807	1.3783	1.363	1.3515	1.34578
C_4S_5	1.755	1.7353	1.744	1.7392	1.74413
S_5C_1	1.7348	1.7567	1.713	1.7252	1.72974
C_4C_6	1.4483	1.4508	1.447	1.4647	1.47824

^{b} = solid-state x-ray data , ^{c} = gas phase electron diffraction measurement

The C_1C_2, and C_3C_4 bond lengths of neutral bithiophene molecule calculated in this work are in close agreement with the experimental results but these bonds are underestimated by UB3-PW91/cc-pVDZ level of calculation [17].

5.1.2.3 Terthiophene

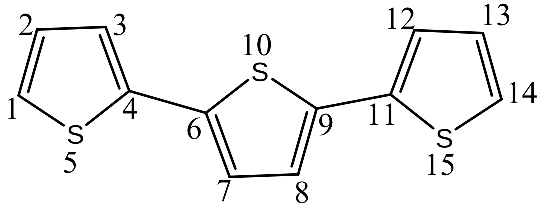

Table 9. Bond length of neutral trithiophene molecule

Parameter	This work (DFT/3-21G*)	This work (DFT/6-31G*)	[17] UB3-PW91/cc-pVDZ
C_1C_2	1.37010	1.3675	1.37
C_2C_3	1.42722	1.4231	1.42
C_3C_4	1.38147	1.3796	1.403
C_4S_5	1.75635	1.7355	1.756
S_5C_1	1.73423	1.7582	1.712
C_4C_6	1.44400	1.44678	1.415
C_6C_7	1.38171	1.37936	1.381
C_7C_8	1.41877	1.41583	1.414
C_8C_9	1.38171	1.37936	1.381
C_9C_{10}	1.75531	1.75748	1.749

5.1.2.4 Longer Oligothiophenes

Table 10 contains the optimized structural parameters obtained in this work at the B3LYP/6-31G* with published results obtained at the same level of theory.

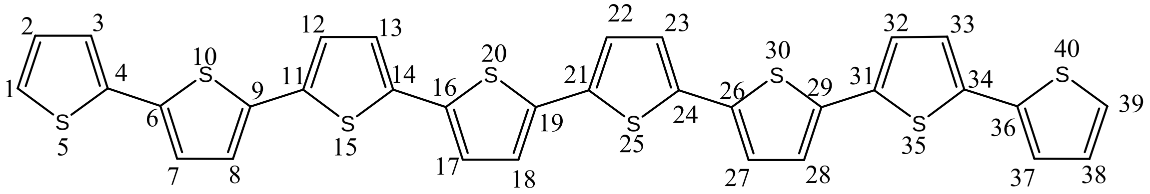

Table 10. Optimized bond lengths (in Å) of oligothiophenes in neutral state compared with results from ref.22 both obtained at **B3LYP/6-31G*** level.

Parameter	Number of thiophene rings								
	1	1,Exp[18]	2	2. [22]	2. Exp.[18]	2Exp[33]	3	3,[22]	3Exp[41]
C_1C_2	1.3674	1.3696	1.3672	1.367	1.350	1.3444	1.3675	1.368	1.347
C_2C_3	1.4298	1.4232	1.4235	1.424	1.413	1.4336	1.4231	1.423	1.433
C_3C_4	1.3674	1.3696	1.3783	1.378	1.363	1.3515	1.3796	1.379	1.355
C_1S_5	1.7356	1.7140	1.7353	1.736	1.744	1.7392	1.7355	1.735	1.721
C_4S_5	1.7356	1.7140	1.7567	1.756	1.713	1.7252	1.7582	1.757	1.738
C_4C_6	-	-	1.4508	1.451	1.447	1.4647	1.44678	1.448	1.454
C_6C_7	-	-	1.3783	-	-		1.37936	1.379	1.354
C_7C_8	-	-	1.4235	-	-	-	1.41583	1.417	1.427
C_8C_9	-	-	1.3672	-	-	-	1.37936	-	-
C_6S_{10}	-	-	1.7567	-	-	-	1.75748	1.757	1.737
C_9S_{10}	-	-	1.7353	-	-	-	1.75748	-	-
C_9C_{11}	-	-	-	-	-	-	1.44678	-	-
$C_{11}C_{12}$	-	-	-	-	-	-	1.37959	-	-
$C_{12}C_{13}$	-	-	-	-	-	-	1.42306	-	-
$C_{13}C_{14}$	-	-	-	-	-	-	1.36751	-	-
$C_{11}S_{15}$	-	-	-	-	-	-	1.75816	-	-
$C_{14}S_{15}$	-	-	-	-	-	-	1.73553	-	-

The calculated results obtained in this work are in a very close agreement with the reported results obtained at the same level of theory. From both the results it is observed that as the number of thiophene rings increase the corresponding bond lengths of oligothiophenes are consistent and show a very small difference. Up on oxidation the single bonds become shorter and double bonds become longer. This change indicates the emerging of a quinoidal character when an electron is removed from the neutral compounds.

Table11. Optimized bond lengths (in Å) of oligothiophenes in neutral state compared with results from ref.22 both obtained at **B3LYP/6-31G*** level.

Parameter	Number of thiophene rings					
	4	4, [22]	5	5, [22]	6	6, [22]
C_1C_2	1.36779	1.368	1.36769	1.368	1.36769	1.368
C_2C_3	1.42251	1.423	1.42276	1.423	1.42279	1.423
C_3C_4	1.38024	1.380	1.37991	1.380	1.37988	1.380
S_5C_1	1.73588	1.735	1.73532	1.736	1.73539	1.736
C_4S_5	1.75800	1.757	1.75828	1.758	1.75827	1.758
C_4C_6	1.44610	1.447	1.44604	1.446	1.44601	1.446
C_6C_7	1.38060	1.380	1.38028	1.380	1.38032	1.380
C_7C_8	1.41403	1.416	1.41433	1.414	1.41446	1.414
C_8C_9	1.38158	1.381	1.38130	1.381	1.38137	1.381
C_6S_{10}	1.75749	1.757	1.75746	1.758	1.75740	1.757
C_9S_{10}	1.75845	1.758	1.75878	1.759	1.75888	1.759
C_9C_{11}	1.44214	1.443	1.44176	1.442	1.44153	1.441
$C_{11}C_{12}$	1.38158	-	1.38175	1.382	1.38197	1.382
$C_{12}C_{13}$	1.41403	-	1.41348	1.414	1.41322	1.413
$C_{13}C_{14}$	1.38060	-	1.38175	-	1.38204	1.382
$C_{11}S_{15}$	1.75845	-	1.75867	1.759	1.75878	1.759
$C_{14}S_{15}$	1.75749	-	1.75867	-	1.75895	1.759
$C_{14}C_{16}$	1.44610	-	1.44176	-	1.44098	1.441

For the longer oligothiophenes change in bond lengths is observed at the inner rings and the outer ring bond lengths show a very slight change which indicates the quinoid character is limited at the central thiophene rings of longer oligothiophenes.

Table12. Optimized bond lengths (in Å) of oligothiophenes in neutral state compared with results from ref.22 both obtained at **B3LYP/6-31G*** level.

Parameter	Number of thiophene rings			
	7	7 from [22]	8	8 from [22]
C_1C_2	1.36765	1.368	1.36773	1.368
C_2C_3	1.42285	1.423	1.42251	1.423
C_3C_4	1.37993	1.380	1.38017	1.380
S_5C_1	1.73538	1.736	1.73590	1.736
C_4S_5	1.75822	1.758	1.75799	1.758
C_4C_6	1.44594	1.446	1.44585	1.446
C_6C_7	1.38036	1.380	1.38068	1.380
C_7C_8	1.41433	1.414	1.41382	1.414
C_8C_9	1.38138	1.381	1.38174	1.381
C_6S_{10}	1.75747	1.758	1.75752	1.758
C_9S_{10}	1.75888	1.759	1.75881	1.759
C_9C_{11}	1.44147	1.441	1.44121	1.442
$C_{11}C_{12}$	1.38204	1.382	1.38243	1.382
$C_{12}C_{13}$	1.41316	1.413	1.41259	1.413
$C_{13}C_{14}$	1.38217	1.382	1.38252	1.382
$C_{11}S_{15}$	1.75868	1.759	1.75868	1.759
$C_{14}S_{15}$	1.75901	1.759	1.75903	1.759
$C_{14}C_{16}$	1.44073	1.441	1.44048	1.441
$C_{16}C_{17}$	1.38232	1.382	1.38273	1.382
$C_{17}C_{18}$	1.41283	1.413	1.41228	1.413
$C_{18}C_{19}$	1.38232	-	1.38276	1.382
$C_{16}S_{20}$	1.75898	1.759	1.75895	1.759

Table13. Optimized bond lengths (in Å) of oligothiophenes in polaronic (oxidized) states compared with results from ref.22 both obtained at **B3LYP/6-31G***

Parameter	Number of thiophene rings							
	1	1,[22]	2	2,[22]	3	3,[22]	4	4, [22]
C_1C_2	1.4238	-	1.3957	1.396	1.3851	1.385	1.3799	1.380
C_2C_3	1.3798	-	1.3914	1.391	1.4014	1.401	1.4072	1.407
C_3C_4	1.4238	-	1.4161	1.416	1.4031	1.403	1.3957	1.396
C_4S_5	1.7317	-	1.7698	1.770	1.7654	1.765	1.7623	1.762
C_1S_5	1.7317	-	1.7152	1.715	1.7183	1.718	1.7214	1.721
C_4C_6	-	-	1.4059	1.406	1.4138	1.414	1.4224	1.422
C_6C_7	-	-	1.4161	-	1.4137	1.414	1.4073	1.407
C_7C_8	-	-	1.3914	-	1.3819	1.382	1.3866	1.387
C_8C_9	-	-	1.3957	-	1.4137	-	1.4086	1.409
C_6S_{10}	-	-	1.7698	-	1.7578	1.758	1.7539	1.754
C_9S_{10}	-	-	1.7152	-	1.7578	-	1.7623	1.762
C_9C_{11}	-	-	-	-	1.4138	-	1.4092	1.409
$C_{11}C_{12}$	-	-	-	-	1.4031	-	1.4086	-
$C_{12}C_{13}$	-	-	-	-	1.4014	-	1.3866	-
$C_{13}C_{14}$	-	-	-	-	1.3851	-	1.4073	-
$C_{11}S_{15}$	-	-	-	-	1.7654	-	1.7623	-
$C_{14}S_{15}$	-	-	-	-	1.7183	-	1.7539	-
$C_{14}C_{16}$	-	-	-	-	-	-	1.4224	-

Table 14. Optimized bond length (in Å) of oligothiophenes in polaronic (oxidized) states compared with results from ref.22 both obtained at **B3LYP/6-31G***

Parameter	Number of thiophene rings							
	5	5,[22]	6	6,[22]	7	7,[22]	8	8,[22]
C_1C_2	1.3373	1.337	1.3749	1.375	1.37347	1.373	1.3725	1.372
C_2C_3	1.4111	1.411	1.4133	1.413	1.41503	1.415	1.4163	1.416
C_3C_4	1.3911	1.391	1.3888	1.389	1.38692	1.387	1.3856	1.386
C_4S_5	1.7610	1.760	1.7594	1.759	1.75890	1.759	1.7585	1.758
S_5C_1	1.7240	1.724	1.7255	1.726	1.72695	1.727	1.7281	1.728
C_4C_6	1.4270	1.428	1.4321	1.432	1.43480	1.435	1.4368	1.437
C_6C_7	1.4019	1.402	1.3979	1.398	1.39481	1.395	1.3925	1.392
C_7C_8	1.3918	1.392	1.3957	1.396	1.39869	1.399	1.4011	1.401
C_8C_9	1.403	1.403	1.3984	1.398	1.39514	1.395	1.3927	1.393
C_6S_{10}	1.753	1.753	1.7523	1.752	1.75252	1.752	1.7528	1.753
C_9S_{10}	1.762	1.762	1.7619	1.762	1.76137	1.761	1.7608	1.761
C_9C_{11}	1.4128	1.413	1.4178	1.418	1.42168	1.422	1.4248	1.425
$C_{11}C_{12}$	1.4067	1.407	1.4044	1.404	1.40127	1.401	1.3986	1.399
$C_{12}C_{13}$	1.3868	1.387	1.3897	1.390	1.39277	1.393	1.3955	1.395
$C_{13}C_{14}$	-	-	1.4042	1.404	1.40071	1.401	1.3978	1.398
$C_{11}S_{15}$	1.7602	1.760	1.7583	1.758	1.75722	1.757	1.7567	1.757
$C_{14}S_{15}$	-	-	1.7614	1.761	1.76163	1.762	1.7614	1.761
$C_{14}C_{16}$	-	-	1.4139	1.414	1.41673	1.417	1.4198	1.420
$C_{16}C_{17}$	-	-	-	-	1.40280	1.403	1.4007	1.401
$C_{17}C_{18}$	-	-	-	-	1.39087	1.391	1.3931	1.393
$C_{18}C_{19}$	-	-	-	-	1.40280	-	1.40033	1.400
$C_{16}C_{20}$	-	-	-	-	1.76016	1.760	1.75911	1.759

5.1.3 3-(2,5-dialkoxyphenyl) thiophenes

In addition to the thiophene oligomers the dialkoxyphenyl thiophenes were investigated with the same methods and procedures as of the oligothiophenes. In the structures the R-group represents butyloxy, heptyloxy and octyloxy groups. The structural parameters obtained at the DFT/B3LYP/ 3-21G* levels are listed in tables 15, 16 and 17. The numbering system followed for the dialkoxyphenyl thiophenes is as follows:

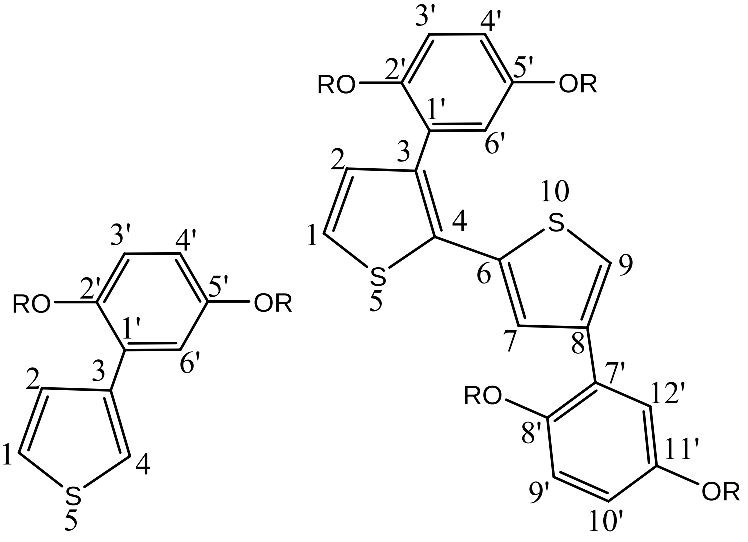

Table15. Optimized bond length (in Å) of monomer and dimmer of DBOPT in neutral (reduced) and polaronic (oxidized) states obtained at **B3LYP/3-21G*** level.

Parameter	Monomer of DBOPT		Dimmer of DBOPT	
	Red	Oxd	Red	Oxd
C_1C_2	1.36482	1.36220	1.36455	1.36727
C_2C_3	1.44565	1.44754	1.44095	1.43200
C_3C_4	1.37881	1.39649	1.38697	1.41183
C_4S_5	1.72892	1.70625	1.75377	1.75631
S_5C_1	1.73709	1.74154	1.73276	1.73051
C_4C_6	-	-	1.45632	1.43170
C_6C_7	-	-	1.37471	1.38744
C_7C_8	-	-	1.43890	1.42346

Table15. Continued

C_8C_9	-	-	1.38007	1.40305
C_9S_{10}	-	-	1.72491	1.70554
C_6S_{10}	-	-	1.75435	1.76956
C_3-$C_{1'}$	1.47933	1.45715	1.48135	1.46704
C1’-C2’	1.41881	1.45545	1.41713	1.43097
$C_{2'}$-O	1.39098	1.33910	1.39053	1.36946
C2’C3’	1.39240	1.41696	1.39189	1.39668
C3’-C4’	1.39827	1.37135	1.39869	1.39114
C4’-C5’	1.39291	1.42770	1.39335	1.40481
$C_{5'}$-O	1.38926	1.34387	1.38946	1.37368
C5’-C6’	1.40012	1.40551	1.40088	1.39827
C6’-C1’	1.39533	1.38760	1.39364	1.39717
C_8-$C_{7'}$	-	-	1.47907	1.46560
$C_{8'}$-O	-	-	1.39035	1.36972
$C_{11'}$-O	-	-	1.38994	1.36897

The C_1C_2 bond length in all of the three monomers, DBOPT, DHOPT, and DOOPT, decreased up on the removal of an electron, table 15. However, similar bond, C_1C_2, of a thiophene monomer has a length of 1.3697Å at the reduced state and this bond increased to 1.43107Å for the case of oxidized thiophene monomer, table 3 above This difference is due to the introduction of phenyl on the thiophene monomer. In the other case the introduction of dialkoxy substituents on the thiophene ring delocalized the radical and the cation toward the oxygen atoms of the alkoxy substituents. The bond lengths of C_1C_2, C_4S_5, and C_3C_4 increased, again that shows the formation of single bonds. In this case the removed electron is from the C_3C_4 double bond since it is changed to single bond after the oxidation process and C_1C_2 is still double bond in the oxidized form.

Table16. Optimized bond length in (Å) of DAOPT in neutral (reduced) and polaronic (oxidized) states obtained at **B3LYP/3-21G*** level.

Parameter	Monomer of DHOPT		Dimmer of DHOPT	
	Red	Oxd	Red	Oxd
C_1C_2	1.36480	1.36230	1.36448	1.36699
C_2C_3	1.44557	1.44737	1.44073	1.43272
C_3C_4	1.37876	1.39625	1.38698	1.41098
C_4S_5	1.72910	1.70645	1.75436	1.75444
S_5C_1	1.73713	1.74148	1.73297	1.73120
C_4C_6	-	-	1.45578	1.43306
C_6C_7	-	-	1.37518	1.38609
C_7C_8	-	-	1.43842	1.42498
C_8C_9	-	-	1.37982	1.40249
C_9S_{10}	-	-	1.72512	1.70519
C_6S_{10}	-	-	1.75466	1.76911
C_3-$C_{1'}$	1.47942	1.45738	1.48148	1.46680
$C_{2'}$-O	1.39146	1.33915	1.39017	1.36952
$C_{5'}$-O	1.38950	1.34385	1.38974	1.37334
C_8-$C_{7'}$	-	-	1.47887	1.46554
$C_{8'}$-O	-	-	1.39045	1.36931
$C_{11'}$-O	-	-	1.39001	1.36864

The interring bond length decreased which indicates the formation of a double bond after the removal of the electron. In the case of phenyl ring, $C_{1'}C_{2'}$, $C_{2'}C_{3'}$, $C_{4'}C_{5'}$, $C_{5'}C_{6'}$ became more lengthened, and $C_{2'}O$, $C_{5'}O$ bond lengths decreased which indicates a double bond. Depending on these observations the following scheme is proposed for the structure of the neutral and oxidized form of the monomers.

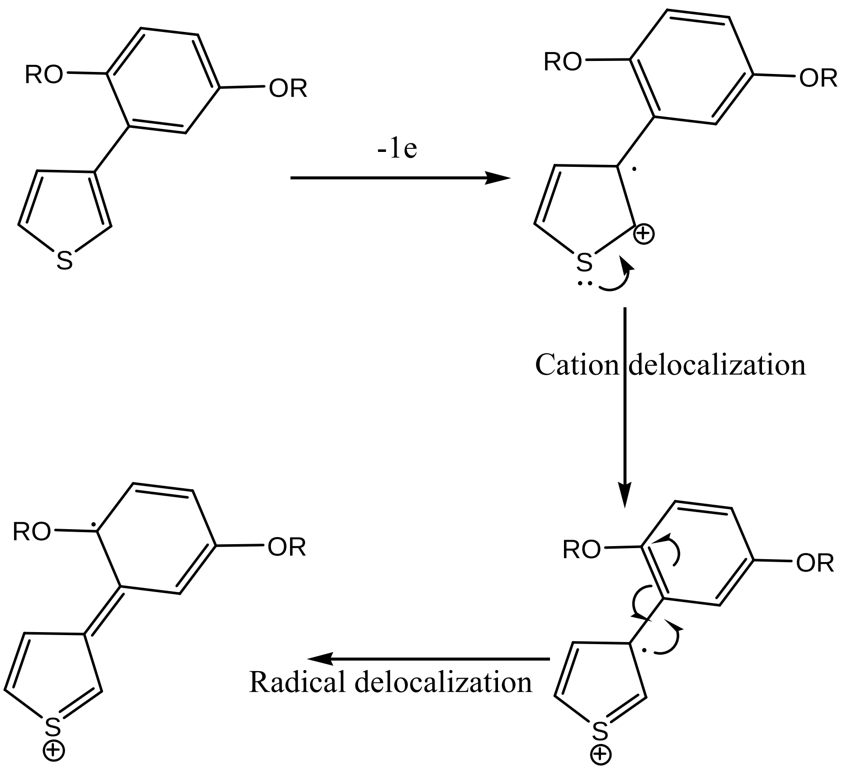

Scheme 8. Charge delocalization in the monomers of dialkoxyphenylthiophenes

Table17. Optimized bond lengths (in Å) of DAOPT in neutral (reduced) and polaronic (oxidized) states obtained at **B3LYP/3-21G*** level.

Parameter	Monomer of DOOPT	
	Red	Oxd
C_1C_2	1.36481	1.36235
C_2C_3	1.44557	1.44727
C_3C_4	1.37874	1.39610
C_4S_5	1.72903	1.70655
S_5C_1	1.73719	1.74145
C_4C_6	-	-
C_6C_7	-	-
C_7C_8	-	-

Table17. Continued

C_8C_9	-	-
C_9S_{10}	-	-
C_6S_{10}	-	-
C_3-$C_{1'}$	1.47939	1.45745
$C_{2'}$-O	1.39145	1.33883
$C_{5'}$-O	1.38946	1.34364
C_8-$C_{7'}$	-	-
$C_{8'}$-O	-	-
$C_{11'}$-O	-	-

In the oxidized state the phenyl ring has lost its aromatic character and this is the major factor for the unstability of the oxidized form compared with the neutral compounds since the change in Gibbs free energy is positive for all the cases. Considering the dimmers, for all the three dimmers bond lengths of C_1C_2, C_3C_4, C_4S_5, C_6S_{10}, C_6C_7 and C_8C_9 all increased and bond lengths of C_1S_5, C_2C_3, C_4C_6, C_7C_8, and C_9S_{10} all decreased which suggests that single bond character for the former bonds and double bond character for the later bonds. All the interring bonds changed to double bonds and the results indicate that the electron is removed from C_1C_2 double bond since its length increased. Based on these observations the structure of the neutral and oxidized species of the dimmers is proposed by the following scheme:

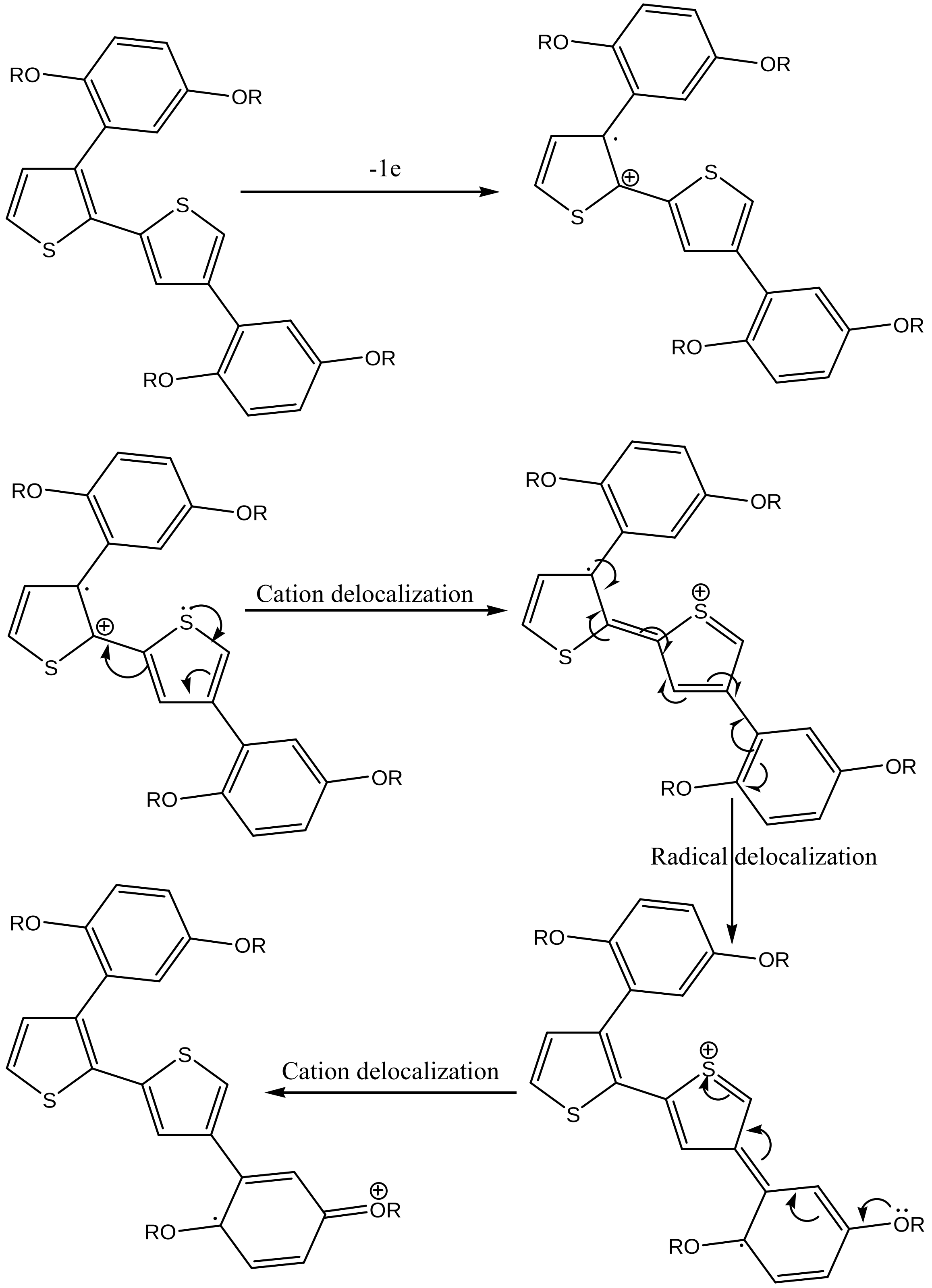

Scheme 9. Delocalization in the dimmers of dialkoxyphenylthiophenes

This change in the structural parameters is observed for all the three dialkoxy phenyl substituted thiophenes, except that there is a slight change in bond lengths caused on both the neutral and oxidized forms with increase in the chain length of the side alkoxy substituents. In this case the C-C bond lengths of the thiophene ring decreased and C-S bond lengths increased with the increase in the alkoxy chain lengths. In the other case the interring and C-O bond lengths increased with the increase in the chain lengths of the alkoxy substituents. The C-O bond lengths decreased up on oxidation of the compounds.

Table 18. Bond lengths (in Å) of the monomers as calculated by **DFT/B3LYP/3-21G***

Parameter	Monomers of 3-(2,5-dialkoxyphenyl) thiophenes					
	DBOPT		DHOPT		DOOPT	
	Red	Oxd	Red	Oxd	Red	Oxd
C_1C_2	1.36482	1.36220	1.36480	1.36230	1.36481	1.36235
C_2C_3	1.44565	1.44754	1.44557	1.44737	1.44557	1.44727
C_3C_4	1.37881	1.39649	1.37876	1.39625	1.37874	1.39610
C_4S_5	1.72892	1.70625	1.72910	1.70645	1.72903	1.70655
S_5C_1	1.73709	1.74154	1.73713	1.74148	1.73719	1.74145
C_3-$C_{1'}$	1.47933	1.45715	1.47942	1.45738	1.47939	1.45745
$C_{2'}$-O	1.39098	1.33910	1.39146	1.33915	1.39148	1.33883
$C_{5'}$-O	1.38926	1.34387	1.38950	1.34385	1.38951	1.34364

The C-C and C-O bond lengths of the monomers and their dimmers show a very small difference in both reduced states. The effect of the alkoxy chain length is observed on the C-O bond lengths even if the difference is small. $C_{2'}$-O in the neutral DBOPT has a length of 1.39098 Å, but for DHOPT in the same state has a length of 1.39146 Å and for DOOPT 1.39148 Å, table 18. The $C_{5'}$-O bond length has also increased up on increasing the alkoxy chain length. For both the monomers and dimmers C-O bond lengths became shorter up on the removal of an electron, which shows the partial double bond character of the bonds.

5. 2 Charges on Atoms

5.2.1 Thiophenes

As shown in table19 up on oxidation of the oligothiophene molecules, the Mulliken charges on the sulfur atoms became more positive at the oxidized species (0.254 to 0.518 for S_1 of thiophene for example). This condition is observed for all the oligothiophene molecules. The charges on the carbon atoms show a different change, some of them decreased and others increased.

Table19. Charge on atoms calculated at the **B3LYP/6-31G*** level.

Atom no.	Thiophene		Bithiophene		Terthiophene		Tetrathiophene	
	Red	Oxd	Red	Oxd	Red	Oxd	Red	Oxd
C_1	-0.346	-0.250	-0.344	-0.289	-0.343	-0.305	-0.342	-0.315
C_2	-0.096	-0.059	-0.097	-0.084	-0.098	-0.090	-0.097	-0.092
C_3	-0.096	-0.059	-0.144	-0.100	-0.143	-0.109	-0.142	-0.116
C_4	-0.346	-0.250	-0.145	-0.139	-0.158	-0.166	-0.157	-0.169
S_5	0.254	0.518	0.261	0.417	0.263	0.376	0.264	0.351
C_6	-	-	-0.145	-0.139	-0.134	-0.114	-0.132	-0.111
C_7	-	-	-0.144	-0.100	-0.149	-0.122	-0.158	-0.131
C_8	-	-	-0.097	-0.084	-0.149	-0.122	-0.148	-0.122
C_9	-	-	-0.344	-0.289	-0.134	-0.144	-0.146	-0.147
S_{10}	-	-	0.261	0.417	0.265	0.369	0.267	0.348
C_{11}	-	-	-	-	-0.156	-0.106	-0.146	-0.142
C_{12}	-	-	-	-	-0.143	-0.109	-0.148	-0.121
C_{13}	-	-	-	-	-0.098	-0.090	-0.150	-0.131
C_{14}	-	-	-	-	-0.343	-0.365	-0.132	-0.141
S_{15}	-	-	-	-	0.263	0.376	0.267	0.348

Table19.Continued

Atom no.	Pentathiophene		Hexathiophene		Heptathiophene		Octathiophene	
	Red	Oxd	Red	Oxd	Red	Oxd	Red	Oxd
C_1	-0.342	-0.323	-0.342	-0.324	-0.342	-0.327	-0.342	-0.329
C_2	-0.098	-0.094	-0.097	-0.095	-0.097	-0.095	-0.097	-0.096
C_3	-0.143	-0.123	-0.142	-0.124	-0.142	-0.127	-0.142	-0.129
C_4	-0.157	-0.167	-0.157	-0.168	-0.167	-0.177	-0.157	-0.166
S_5	0.264	0.323	0.264	0.323	0.265	0.314	0.265	0.309
C_6	-0.132	-0.115	-0.132	-0.116	-0.132	-0.117	-0.132	-0.119
C_7	-0.158	-0.148	-0.156	-0.148	-0.156	-0.142	-0.159	-0.143
C_8	-0.148	-0.125	-0.147	-0.126	-0.147	-0.129	-0.147	-0.131
C_9	-0.146	-0.156	-0.147	-0.157	-0.147	-0.153	-0.147	-0.154
S_{10}	0.267	0.323	0.267	0.324	0.268	0.316	0.268	0.310
C_{11}	-0.144	-0.132	-0.144	-0.133	-0.144	-0.133	-0.144	-0.133
C_{12}	-0.148	-0.132	-0.148	-0.133	-0.144	-0.135	-0.144	-0.131
C_{13}	-0.148	-0.127	-0.148	-0.128	-0.148	-0.129	-0.143	-0.131
C_{14}	-0.144	-0.146	-0.144	-0.147	-0.145	-0.146	-0.145	-0.148
S_{15}	0.268	0.324	0.268	0.325	0.269	0.318	0.269	0.312

The charges on the carbon atoms of thiophene and bithiophene both increased after oxidation and became more positive. This shows the cation formed after the removal of an electron is delocalized on both the carbon atoms. This condition is different for the case of oligomers next to bithiophene. The charges on C_4, C_9 and C_{14} of oligomers from terthiophene to octathiophene have decreased and became more negative (for example C_4 = has decreased from -0.158 to -0.166, table 19). This change in the Mulliken charges indicates that carbon atoms at 4, 9, and 14 positions are more responsible for carrying the radical or the odd electron. The other carbon atoms show an increase in the Mulliken charges and became more positive at the oxidized species. This indicates that the cation is delocalizing at carbon atoms other than C_4, C_9 and C_{14}. Based on this observation the following diagrammatic representation for the delocalization of the radical can be proposed.

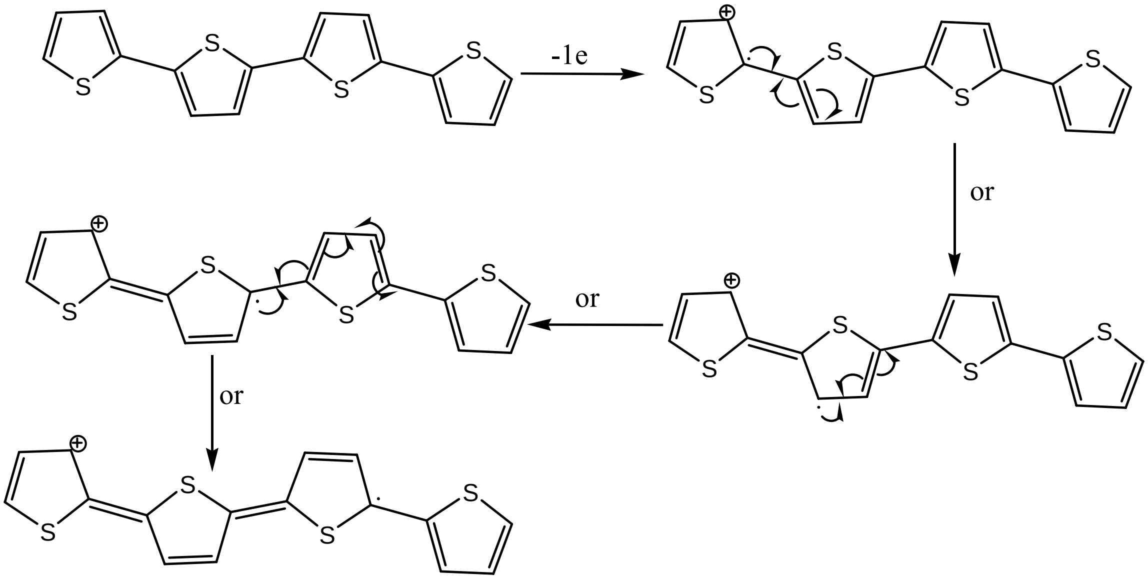

Scheme 10. Radical delocalization in oligothiophenes

The charges on the sulfur atoms became more positive after the removal of the electron from the neutral molecules. This increase in charge of sulfur atoms is due to the delocalization of the positive charge on sulfur atoms in addition to the delocalization on the carbon atoms. The change in the charges observed on the sulfur atoms is very much greater than the change in charge of the carbon atoms. The following scheme can represent the delecalization of the positive charge on the carbon and sulfur atoms.

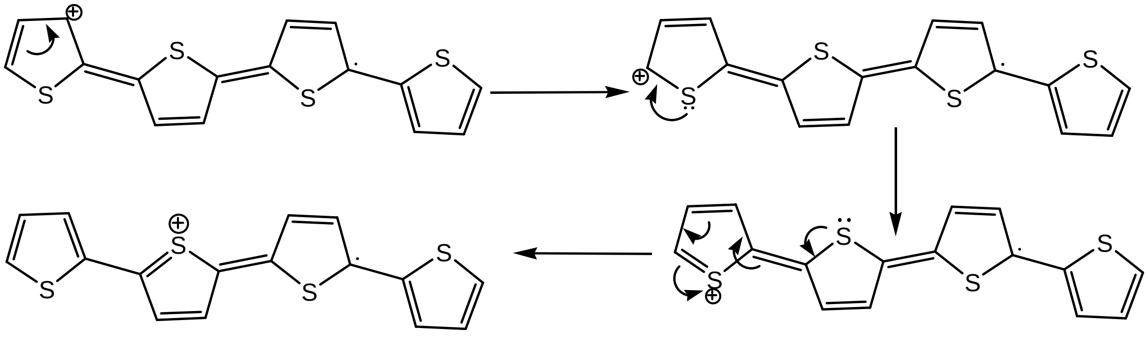

Scheme 11. Charge delocalization in oligothiophenes

5.2.2 3-(2,5-dialkoxyphenyl) thiophenes

The Mulliken charges obtained from the three monomers and their dimmers are listed in tables 20 and 21. From the Mulliken charges of the monomers it is observed that the cation can delocalize on all the carbons since their charges became more positive up on oxidation.

Table 20. Mulliken charges for the monomers of DBOPT, DHOPT, and DOOPT calculated by **DFT/B3LYP/3-21G***

Atom number	DBOPT		DHOPT		DOOPT	
	Reduced	Oxidized	Reduced	Oxidized	Reduced	Oxidized
C_1	-0.436	-0.428	-0.436	-0.428	-0.436	-0.428
C_2	-0.160	-0.151	-0.160	-0.151	-0.160	-0.151
C_3	0.025	0.021	0.025	0.020	0.025	0.020
C_4	-0.427	-0.407	-0.427	-0.407	-0.427	-0.407
S_5	0.393	0.522	0.393	0.521	0.393	0.521
$C_{1'}$	-0.054	-0.037	-0.054	-0.032	-0.054	-0.032
$C_{2'}$	0.307	0.387	0.307	0.387	0.307	0.387
$C_{3'}$	-0.209	-0.188	-0.209	-0.188	-0.209	-0.188
$C_{4'}$	-0.218	-0.181	-0.218	-0.182	-0.218	-0.182
$C_{5'}$	0.314	0.378	0.314	0.378	0.314	0.378
$C_{6'}$	-0.206	-0.189	-0.206	-0.190	-0.205	-0.190

It is also observed that the phenyl and the alkoxy substituents made the carbon atoms, at which they are attached, more positive than the other carbon atoms. This indicate the electron withdrawing property of the alkoxy and phenyl substituents. The other information obtained from the charges is that the length of the alkoxy substituents has a negligible effect on the charges of the carbon and sulfur atoms. These observations are in a very good agreement with the structures proposed for the monomers and dimmers based on the structural parameters.

Table 21. Mulliken charges for dimmers calculated by **DFT/B3LYP/3-21G***

Atom number	Dimmer of DBOPT		Dimmer of DHOPT	
	Charge		Charge	
	Reduced	Oxidized	Reduced	Oxidized
C_1	-0.440	-0.420	-0.440	-0.421
C_2	-0.151	-0.139	-0.149	-0.140
C_3	0.040	0.047	0.039	0.047
C_4	-0.260	-0.241	-0.258	-0.242
S_5	0.423	0.484	0.422	0.484
C_6	-0.277	-0.259	-0.275	-0.261
$C_{7'}$	-0.160	-0.164	-0.161	-0.163
C_8	0.031	0.032	0.032	0.032
C_9	-0.435	-0.409	-0.435	-0.409
C_{10}	0.456	0.548	0.457	0.546

The change in charges on carbon atoms at position 1 and 2 in both the monomers and dimmers is different, for example from table 21 for the dimmer of DBOPT the charge of C_1 is –0.440 in the neutral form and –0.420 in the oxidized form (a difference of 0.02), but the charge of the carbon atom at position 2 of dimmer of DBOPT is –0.151 in its neutral form and –0.139 in its oxidized state (a difference of 0.012). Again the charge on carbon atom 3 before oxidation is 0.040 and 0.047 after oxidation, which has a difference of 0.007, whereas for carbon number 4 charges before oxidation is –0.260 and –0.241 after oxidation with a difference of 0.019. From these results it is observed that carbon 1 and 4 are responsible for carrying the cation. In the other case the change is very small for carbon 3 when compared with carbon 2. These evidences show that when the electron is removed the cation will be formed at carbon atom 4 and the odd electron at carbon atom 3, which agrees with the results obtained from the structural parameters.

5.3 UV-Visible Absorption Wavelengths

The electronic spectra involving transition of valence electrons that occur in the UV-visible region was studied computationally in order to investigate the effect of length of conjugation and chain length of the substituents using B3LYP/3-21G* and B3LYP/6-31G* levels. Table 22 contains the calculated absorption λ_{max} and excitation energy for the thiophene oligomers and the 3-(2,5-dialkoxyphenyl) thiophenes.

Table 22. Calculated excitation energy and absorption wavelength of oligothiophenes and dialkoxyphenyl thiophenes

Compounds	TD-DFT/B3LYP/3-21G*		TD-DFT/B3LYP/6-31G*	
	λ_{max} /nm/	Excitation energy /ev/	λ_{max} /nm/	Excitation energy /ev/
Thiophene	203.29	6.0989	206.69	5.9985
Bithiophene	299.37	4.1415	307.65	4.0300
Terthiophene	369.02	3.3598	379.37	3.2682
Tetrathiophene	424.56	2.9203	436.90	2.8378
Pentathiophene	469.72	2.6396	482.36	2.5703
Hexathiophene	507.75	2.4419	520.22	2.3833
Heptathiophene	536.73	2.3100	551.51	2.2481
Octathiophene	561.72	2.2072	578.54	2.1431
DBOPT	292.84	4.2339	-	-
Dimmer of DBOPT	331.08	3.7448	-	-
DHOPT	292.99	4.2317	-	-
Dimmer of DHOPT	332.92	3.7242	-	-
DOOPT	293.00	4.2316	-	-

From table 22 it is observed that the thiophene monomer is absorbing at a shorter wavelength range and it shows that it is colorless, while with increase in the number of thiophene rings in the oligomers the absorption wavelength increases to the visible range, which indicates the longer oligomers are colored. The results show that as the chain length of the oligothiophene units increase the maximum absorption wavelength increases. Conversely with increase in the chain length the excitation energy decreases which shows increase in the ease of removing electrons from the longer oligothiophenes.

The λ_{max} of the dialkoxyphenyl thiophenes is also calculated using DFT/B3LYP/3-21G* and listed in table 22. From the results obtained it is observed that the three monomers DBOPT, DHOPT, and DOOPT absorb almost at equal wavelength range. When these monomers dimerize the wavelength shifts to longer wavelength range that shows with polymerization the compounds will become colored.

5.4 Band Gaps

The band gaps of the oligothiophenes and the 3-(2,5-dialkoxyphenyl) thiophenes are calculated using DFT/B3LYP/3-21G* and DFT/B3LYP/6-31G* levels of theory. The band gap is obtained by subtracting the energy of the highest occupied molecular orbitals from the energy of the lowest unoccupied molecular orbital (E_{LUMO}-E_{HOMO}). For the oligothiophenes the band gaps are compared with some reported experimental and theoretical results in tables 23, 24, 25, and 26.

Table 23 contains the HOMO, LUMO, and band gap energies of oligothiophenenes obtained in this work.

Table 23. Calculated band gaps obtained at the **B3LYP/6-31G*** in this work

Compounds	Neutral form			Polaronic form		
	HOMO	LUMO	Eg	HOMO	LUMO	Eg
Thiophene	-6.3346	-0.2054	6.1292	-13.300	-7.5346	5.7654
Bithiophene	-5.4742	-1.2438	4.2304	-11.6338	-8.7142	2.9196
Trithiophene	-5.1365	-1.6874	3.4491	-10.1646	-7.8217	2.3429
Tetrathiophene	-4.9599	-1.9336	3.0263	-9.0909	-7.2821	1.8088
Pentathiophene	-4.8616	-2.0803	2.7813	-8.3645	-6.9043	1.4602
Hexathiophene	-4.7974	-2.1813	2.6161	-7.8402	-6.647	1.1932
Heptathiophene	-4.7536	-2.2531	2.5005	-7.4416	-6.4516	0.99
Octathiophene	-4.7193	-2.3092	2.4101	-7.1278	-6.29976	0.828

From the results it is observed that with increase in the number of thiophene units the band gap decreases for both the oxidized and reduced oligommers. In table 24 the band gaps of thiophene oligommers calculated by S. M. Bouzzine et al. [22], which are obtained at the same level of theory, are listed. In their report they reported by reversing the HOMO and LUMO energies in which they gave the HOMO energy for the LUMO and the LUMO energy for the HOMO energy of the orbital. Hence we reversed the data according to the corresponding energies for both the HOMO and LUMO orbital. From these results it is observed that the result reported [22] is exactly identical with our work. From both the results obtained it is observed that for the shorter oligothipphenes the change in the band gap is larger (for example 1.899 between thiophene and bithiophene) whereas for the longer oligothiophenes the difference is small (for example 0.0904 between heptathiophene and octathiophene). This result shows that for the longer oligothiophenes the band gap seems to be consistent.

Table 24. Calculated band gaps obtained at the **B3LYP/6-31G*** reported in [22]

Compounds	Neutral form			Polaronic form		
	HOMO	LUMO	Eg	HOMO	LUMO	Eg
Bithiophene	-5.52	-1.19	4.32	-11.63	-8.71	2.92
Trithiophene	-5.18	-1.63	3.55	-10.16	-7.81	2.35
Tetrathiophene	-5.00	-1.87	3.13	-9.10	-7.27	1.83
Pentathiophene	-4.86	-2.08	2.78	-8.36	-6.90	1.46
Hexathiophene	-4.79	-2.18	2.61	-7.84	-6.64	1.20
Heptathiophene	-4.75	-2.26	2.49	-7.44	-6.44	1.00
Octathiophene	-4.71	-2.30	2.41	-7.13	-6.29	0.84

Table 25 contains the calculated band gaps with some experimental band gaps. For a neutral bithiophene molecule the calculated band gap is 4.2304ev using B3LYP/6-31G* level whereas the experimental value reported is 4.05ev [46], which are in close agreement. The experimental band gap of hexathiophene is 2.40ev [47] whereas the calculated value is 2.6161ev, which are also in close agreement. The Band gap of neutral octathiophene calculated in this work is 2.4101ev and the experimental value reported is 2.3ev [22]. According to the work of S. M. Bouzzine et al. [22] and U. Salzner [47] the experimental band gap of neutral polythiophenes is 2.0 – 2.3ev. From the calculated values the band gap of octathiophene is 2.4101ev. This shows that for the theoretical investigation of polythiophenes and substituted polythiophenes, octathiophene can be considered as a model molecule.

Table 25. Comparison of calculated band gaps with experimental band gaps.

Compounds	Band gap of neutral		Band gap of polaron		Experimental band gap of neutral forms
	3-21G*	6-31G*	3-21G*	6-31G*	
Thiophene	6.2445	6.1292	5.7768	5.7654	5.23
Bithiophene	4.3084	4.2304	2.8899	2.9196	4.05
Terthiophene	3.5168	3.4491	2.3603	2.3429	-
Pentathiophene	2.835	2.7813	1.4533		-
Hexathiophene	2.6591	2.6161	1.1883	1.1932	2.40
Octathiophene	2.4659	2.4101	0.8218	0.828	(2.0-2.3)[a]

[a] The HOMO-LUMO gap of polythiophene in its neutral form

The following graphs show the relation of band gaps with the number of thiophene rings.

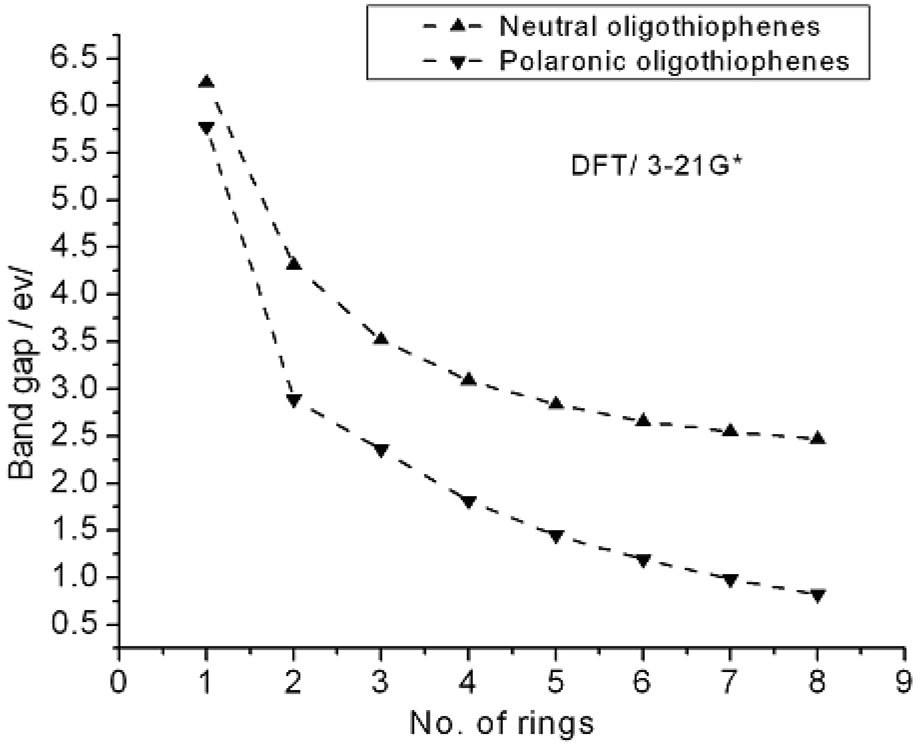

Fig.4 Relation ship between band gaps of oligothiophenes with number of thiophene rings

The graphs also show that further increase in the length of the oligomers has a very little effect on the band gap since the difference in the band gap between two consecutive oligomers is decreasing and for larger oligomers the band gap seems to be constant. When the compounds are oxidized the band gap decreases and also, as the number of rings increases the band gap decreases for the case of oxidized forms. In general from the band gaps calculated it is observed that as conjugation length increases the band gap decreases and for the longer oligothiophenes the band gap change is small compared to shorter oligomers (monomers, and dimmers for example). The band gaps obtained at both 3-21G* and 6-31G* calculation levels show identical change for both the neutral and oxidized states of the oligomers.

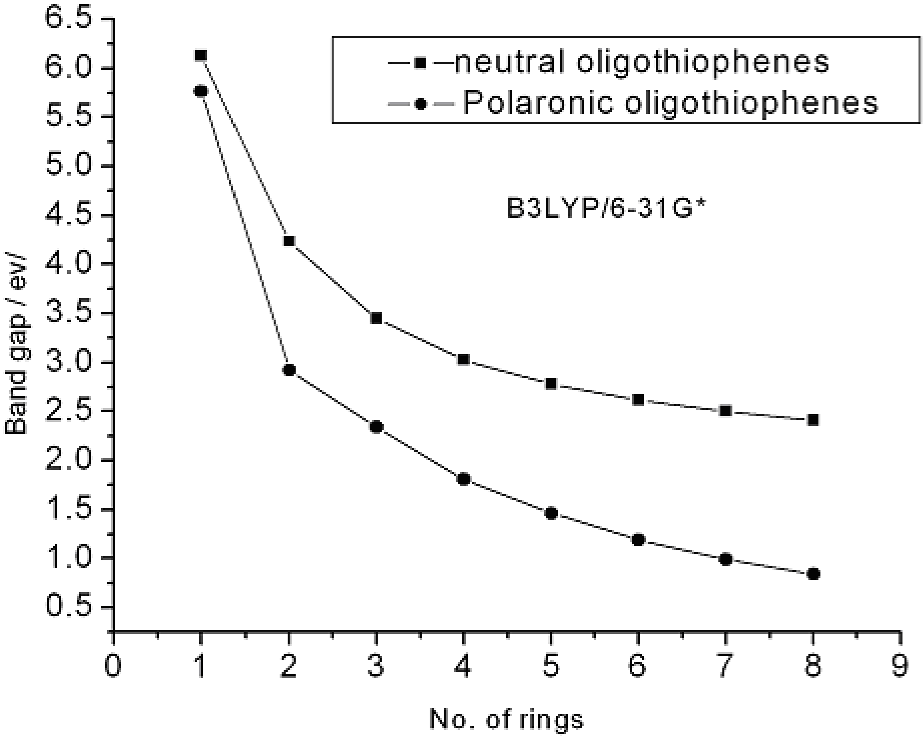

Fig.5 Relationship between band gaps of oligothiophenes with number of thiophene rings

Table 26 contains the HOMO, LUMO, and band gaps of the oligothiophenes and the dialkoxy-substituted phenyl thiophenes. The thiophene monomer has a band gap of 6.2445 ev in its neutral form but the monomer DBOPT has a band gap of 4.7539ev at the same state, which is lower than that of thiophene monomer. The dimmer of DBOPT also has a lower band gap than bithiophene. These results show that the introduction of dialkoxyphenyl substituent at the 3-position of thiophene decreases the band gap.

Table 26. Calculated band gap of oligothiophenes compared with substituted phenyl thiophenes in neutral and polaronic (oxidized) states obtained at **B3LYP/3-21G***

Compounds	Neutral form			Polaronic form		
	HOMO	LUMO	Eg	HOMO	LUMO	Eg
Thiophene	-6.4429	-0.1984	6.2445	-13.4409	-9.6641	3.7768
Bithiophene	-5.5732	-1.2648	4.3084	-11.7674	-8.8775	2.8899
Trithiophene	-5.2347	-1.7179	3.5168	-10.3279	-7.9676	2.3603
Tetrathiophene	-5.0614	-1.9693	3.0921	-9.2353	-7.4187	1.8166
Pentathiophene	-4.9599	-2.1249	2.835	-8.5006	-7.0473	1.4533
Hexathiophene	-4.8910	-2.2319	2.6591	-7.9692	-6.7809	1.1883
Heptathiophene	-4.8537	-2.3026	2.5511	-7.5654	-6.5811	0.9843
Octathiophene	-4.8235	-2.3576	2.4659	-7.2484	-6.4266	0.8218
DBOPT	-5.2105	-0.4566	4.7539	-9.5473	-7.9575	1.5898
Dimm-DBOPT	-4.9907	-0.78392	4.20678	-7.6741	-7.0466	0.6275
DHOPT	-5.1840	-0.4499	4.7341	-9.5139	-7.9211	1.5928
Dimm-DHOPT	-4.9733	-0.7937	4.1796	-7.6497	-7.0117	0.6380
DOOPT	-5.1832	-0.4490	4.7342	-9.5101	-7.9157	1.5944

When the band gaps of the three dialkoxyphenylthiophenes are compared, DBOPT with the shorter alkoxy substituent has a slightly larger band gap than DHOPT and DOOPT. The two monomers, DHOPT, and DOOPT have comparable band gaps. Up on dimmerization the band gaps decrease as it is observed for both the thiophene oligomers and the dialkoxyphenylthiophenes. The oxidized forms of the three monomers and their dimmers show different trend than the neutral forms. The monomer DBOPT in the oxidized form has lower band gap than DHOPT and DOOPT. This is also observed for the dimmers.

5.5 Thermodynamic Properties

To compare the stability of the oligommers at the oxidized states DFT/B3LYP/STO-3G, DFT/B3LYP/3-21G* and HF/STO-3G calculations were carried out for all the compounds and the Gibbs free energy, enthalpy and entropy of the compounds are determined. The change in the thermodynamic properties is calculated by subtracting the thermodynamic properties of the reduced compounds from the thermodynamic properties of the oxidized compounds. The results are listed in tables 27, 28 and 29.

Table 27. Thermodynamic properties of oligomers calculated by **HF/STO-3G**

Compounds	ΔG^0 (Kcal/mol)	ΔH^0 (Kcal/mol)	ΔS^0 (Cal/mol.K)
Thiophene	142.417	143.133	2.399
Bithiophene	110.405	110.146	-0.873
Trithiophene	98.572	97.984	-1.973
Tetrathiophene	92.452	92.076	-1.262
Hexathiophene	89.25576738	88.78136982	-1.592
Heptathiophene	87.521	86.893	-2.104
Octathiophene	86.407	85.596	-2.72
DBOPT	100.607	100.707	0.335
Dimmer of DBOPT	91.141	91.168	0.089
DHOPT	100.141	100.288	0.491
Dimmer of DHOPT	90.672	90.891	0.735
DOOPT	100.032	100.24	0.698
Dimmer of DOOPT	90.490	90.840	1.176

Considering the calculation of thermodynamic properties of all the compounds, the same trend is observed upon polymerization. The monomer units have the largest thermodynamic properties than the dimmers and the trimmers (for example Gibbs free energy of thiophene is 142.417 Kcal/mol and 110.405 Kcal/mol for the dimmer of thiophene calculated by HF/STO-3G in table 27). In other words upon polymerization the change in thermodynamic properties decreases. This decrease in change in thermodynamic properties shows that the oxidized forms of the monomers are unstable when compared with the longer oligomers. The results obtained are plotted for change in Gibbs free energy versus number of thiophene oligomers in figure 6, 7, and 8.

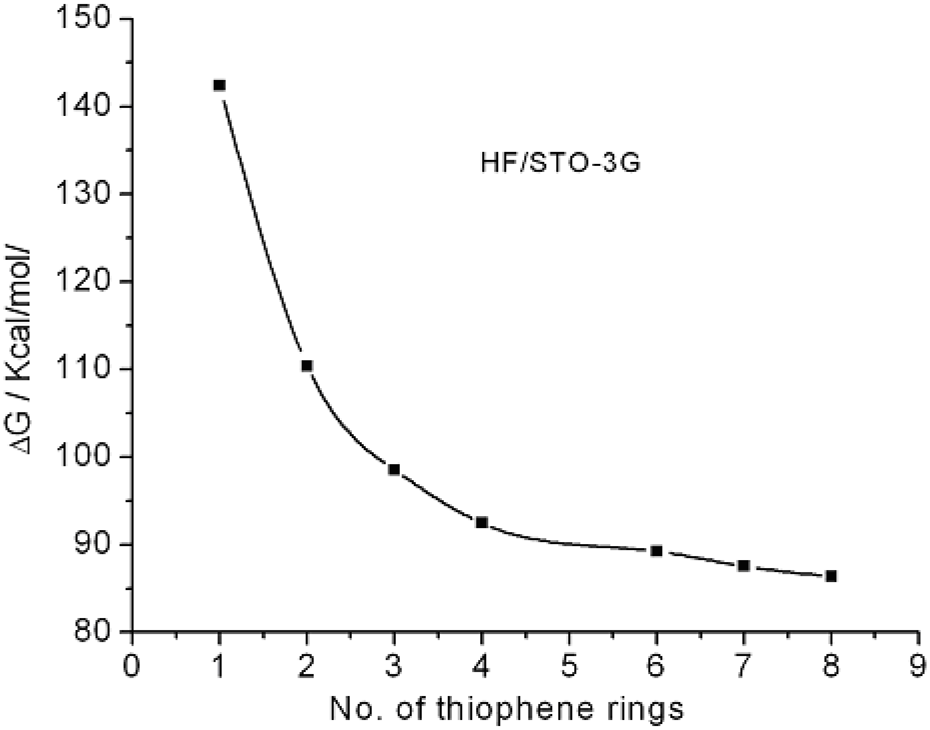

Fig.6 Gibbs free energy of oligothiophenes as a function of numbr of thiophene rings calculated at HF/STO-3G.

The figures show that as the conjugation length increases the stability of the oxidized species increases for both cases. For example the tetrammer of thiophene has a change in Gibbs free energy of 92.452 Kcal/mol, which is less than the dimmer of thiophene with a change in Gibbs free energy of 110.405 Kcal/mol that supports the stability of the radical cation of the tetrammer, table 21. This fact is favored by the delocalization of the radical cation through the longer conjugated molecule that helps to stay for a longer time at the oxidized state. In general as the molecule polymerizes the stability at the oxidized state increases. This case can also be extrapolated to the polymers, in that the highly conjugated polythiophenes and poly (dialkoxyphenyl) thiophenes are stable at the oxidized state than simple polythiophenes and this is may be due to the delocalization of the radical cation through the double bonds.

Table 28. Thermodynamic properties of the oligomers calculated by **DFT/STO-3G**

Compounds	ΔG^0 (Kcal/mol)	ΔH^0 (Kcal/mol)	ΔS^0 (Cal/mol.K)
Thiophene	156.256	157.085	2.782
Bithiophene	120.735	120.622	-0.375
Trithiophene	104.189	104.256	0.223
Tetrathiophene	94.878	94.795	-0.277
Hexathiophene	84.504	84.364	-0.47
Heptathiophene	81.588	81.029	-1.386
Octathiophene	79.052	78.392	-2.213
DBOPT	104.523	104.834	1.044
Dimmer of DBOPT	92.315	92.772	1.533
DHOPT	101.953	102.379	1.431
Dimmer of DHOPT	87.840	87.632	-0.71
DOOPT	101.591	102.067	1.596
Dimmer of DOOPT	87.355	86.982	-1.250

Table 28 and 29 also contain the thermodynamic properties calculated by DFT/B3LYP/STO-3G and DFT/B3LYP/3-21G* levels respectively. The results obtained are in agreement with the results obtained at the HF/STO-3G level.

From tables 27, 28, and 29, we can also see that the dialkoxyphenyl-substituted thiophenes have lower change in Gibbs free energy value than the corresponding thiophenes, which confirms the stability of the dialkoxyphenyl thiophene at the oxidized state. This is may be through hyper conjugative effect. In addition, as the chain length of the alkoxy group increases the stability of the radical cation also increases. The addition of alkoxy side groups helps the dialkoxy phenyl thiophene radical cations to disperse the charge through hyper conjugative effect that is favored by the smaller change in Gibbs free energy.

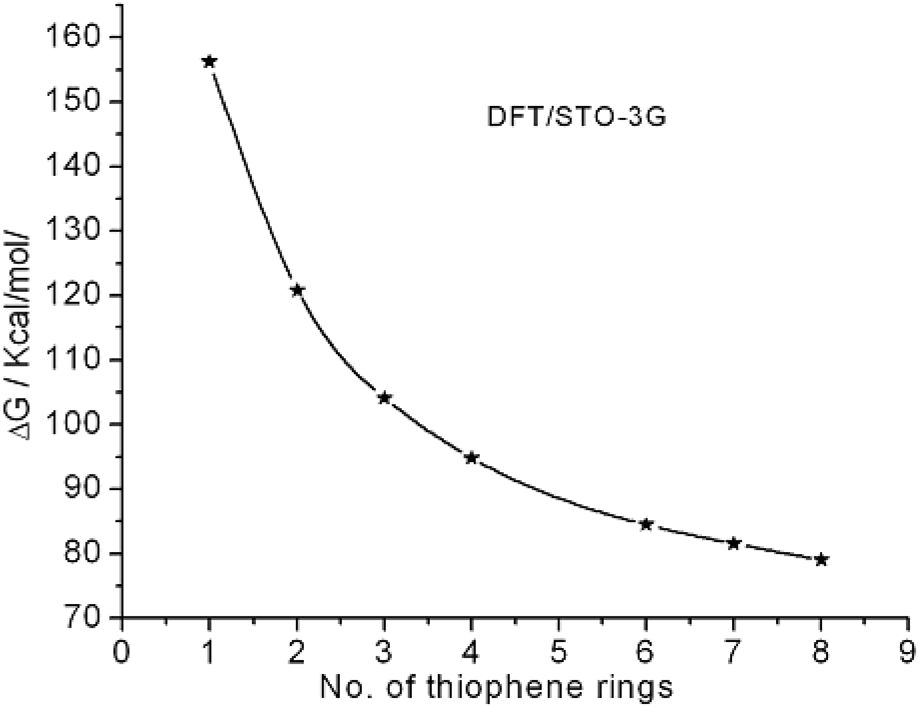

Fig. 7. Gibbs free energy of oligothiophenes as a function of number of thiophene rings calculated at B3LYP/STO-3G.

The oxidized forms of the dimmers are more stable than the monomers. In this case the results can be extrapolated to the polymers in that the polymers have a lower thermodynamic properties compared with the monomers and the oligomers (fig.6, 7, and 8), this indicates the oxidized form of the polymers are more stable than the oligomers due to the large conjugation length which helps the positive charge to delocalize and makes to stay for a longer time at the oxidized state.

Table 29. Thermodynamic properties of the oligomers calculated by **DFT/3-21G***

Compounds	ΔG^0 (Kcal/mol)	ΔH^0 (Kcal/mol)	ΔS^0 (Cal/mol.K)
Thiophene	198.264	198.985	2.419
Bithiophene	165.535	167.328	6.013
Trithiophene	152.716	153.045	1.102
Tetrathiophene	142.513	145.345	9.500
Pentathiophene	137.526	139.971	8.198
Hexathiophene	133.924	136.183	7.577
Heptathiophene	131.668	133.378	5.735
Octathiophene	130.056	131.443	4.652
DBOPT	154.320	154.788	1.59
Dimmer of DBOPT	144.350	145.068	2.411
DHOPT	151.23	152.096	2.905
Dimmer of DHOPT	139.231	140.20	3.251

The three dialkoxy phenyl thiophenes show very small difference in the change in thermodynamic properties calculated by the HF/STO-3G level of theory. But the DFT/B3LYP/STO-3G and DFT/3-21G* levels clearly identified the three monomers and their dimmers. From this change, it is possible to compare their stabilities. DOOPT has the longer alkoxy side attachment and it has the smaller change in Gibbs free energy and it is more stable than DBOPT and DHOPT with shorter alkoxy group and also DHOPT is still more stable than DBOPT at the oxidized state. The dimmers also show similar behavior with the monomers. Thiophene is the least stable dimmer at the oxidized state and dimmer of DOOPT with the longer alkoxy side chain on the phenyl ring is more stable at the oxidized state.

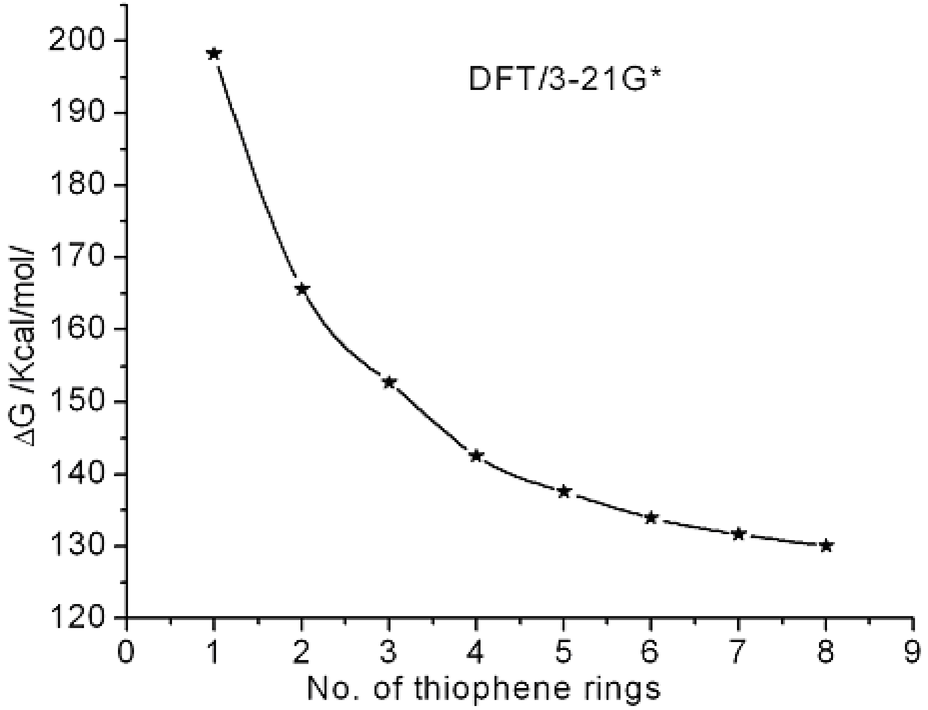

Fig.8 Gibbs free energy of oligothiophenes as a function of number of thiophene rings calculated at B3LYP/3-21G*.

When the polythiophenes and poly (dialkoxyphenyl) thiophenes are compared, the later polymers are more stable at the oxidized state. This stability comes from the substitution of the hydrogen at the 3-position by dialkoxyphenyl substituent. The phenyl ring helps the radical cation to delocalize through the conjugated double bonds and acts as a spacer between the polymer backbones and makes a more rigid backbone that makes a difficult structural reorganization. Due to this, the dialkoxyphenyl-substituted polythiophenes have a higher stability at the oxidized state than the simple polythiophenes.

Conclusion

In this study the thermodynamic and structural properties of oligothiophenes starting from the monomer up to the octammer have been studied. The stability of the oligothiophenes at the oxidized state increases with increase in the number of thiophene rings. The band gap estimations also showed increase in the number of thiophene rings decreases the band gap and improves the conductivity. Oxidation of the neutral oligothiophenes changes the structure from aromatic form to quinoid form. This evidence is also reported in other articles [38,41,51,53]. The quinoid structural character is formed in the inner rings of the thiophene oligomers.

3-(2,5-dibutyloxyphenyl) thiophene (DBOPT), 3-(2,5-diheptyloxyphenyl) thiophene (DHOPT), and 3-(2,5-dioctyloxyphenyl) thiophene (DOOPT) monomers and their dimmers are also studied. The thermodynamic properties showed that DOOPT with the longer alkoxy side chain on the phenyl thiophene is more stable than the two at the oxidized state. DOOPT has also a slightly lower band gap than the two at the reduced state. From the three monomers DOOPT is relatively stable and can better be used for conducting polymer materials.

In addition to the thiophene oligomers and dialkoxyphenylthiophenes we have also investigated the properties of 3,4-dicyanobithiophene (DCNBTH), 3,4-diaminobithiophene (DABTH), 3,4-dibutyloxybithiophene (DBOBTH) and we have compared with properties of bithiophene and dimmer of DBOPT. From all the compounds DBOBTH is more stable and have lower band gap even than the dimmer of DBOPT.

References

[1] R. D. McCullough, *Adv. Mater.,* 10, **1998**, 93-116.

[2] A. S. Ribeiro; W. A. Gazotti; V. C. Nogueira; D. A. Machado; P. F. dos Santos Filho; and M. A. D. Paoli, *J. Chil. Chem. Soc.,* 49, **2004**,197-204.

[3] P. M. S. Monk; R. J. Mortimer; and D. R. Rosseinsky, *Electrochromism, Fundamentals and Applications*, **1995**, VCH Publishers, New York, USA.

[4] S. Admassie; W. Mammo; T. Solomon; T. Yohannes; and M. R. Andersson, *Bull. Chem. Soc. Ethiop.,* 19, **2005**, 1-10.

[5] T. Johansson; W. Mammo; M. R. Andersson; and O. Inganäs, *Chem. Mater.,*11, **1999**, 3133-3139.

[6] Y. Kaminorz; E. Smela; O. Inganäs; and L. Brehmer, *Adv. Mater.,* 10, **1998**, 765-769.

[7] H. W. Heuer; R. Wehrmann; and S. Kirchmeyer, *Adv. Funct. Mater*., 12, **2002**, 89-94.

[8] X. Wang; E. Perzon; W. Mammo; F. Oswald; S. Admassie; N. K. Persson; F. Langa; M. R. Andersson; and O. Inganäs, *Thin Solid Films*, 511/512, **2006**, 576-580.

[9] I. N. Levine, *Quantum Chemistry*, 4th ed., Prentice Hall: Engelwood Cliffs, NJ, **1991**.

[10] J. B. Foresman; Ǽ. Frisch, *Exploring Chemistry with Electronic Structure Methods*; Gaussian Inc: Pittsburgh, **1993**.

[11] F. Jensen, *Introduction to Computational Chemistry*, John Willey and Sons, **2004**.

[12] C. J. Cramer, *Essentials of Computational Chemistry*, 2nd ed., John Willey and Sons, **2004**.

[13] D. A. McQuarrie, *Quantum Chemistry*, Viva Books P. L. C., New Delhi, **2005**.

[14] T. Yohannes, *All-Solid-State Photoelectrochemical Solar Energy Conversion*, Ph. D. Dissertation, Department of Chemistry, Addis Ababa University, **1997**.

[15] M. A. Jean; J. Delhalle; and J. L. Bredas, *Quantum Chemistry Aided Design of Organic Polymers*, World Scientific Publishing, Singapore, **1991**.

[16] H. Lund; and O. Hammerich, *Organic Electrochemistry*, 4th ed., Marcel Dekker Publishers, **2001**.

[17] M. Rubio; E. Orti; R. Pou-Amerigo; and M. Merchan, *J. Phys. Chem. A*, 105, **2001**,

9789-9794.

[18] E. Orti; P. M. Viruela; J. Sánchez-Marin; and F. Tomás, *J. Phys. Chem.,* 99, **1995**, 4955-4963.

[19] M. R. Andersson; O. Thomas; W. Mammo; M. Svensson; M. Theander; and O. Inganäs, *J. Mater. Chem.,* 9, **1999**, 1933-1940.

[20] R. D. McCullough; S. T. Nagle; S. P. Williams; R. D. Lowe; and M. Jayaraman, *J. Am. Chem. Soc.,* 115, **1993**, 4910-4911.

[21] M. J. L. Santos; A. F. Rubira; R. M. Pontes; E. A. Basso; and E. M. Girotto, *J. Solid State Electrochem.,* 10, **2006**, 117-122.

[22] S. M. Buozzine; S. Bouzakraou; M. Bouachrine; and M. Hamidi, *J. Mol. Struct.: THEOCHEM.,* 726, **2005**, 217-276.

[23] M. Belletête; S. Beaupre; J. Bouchard; P. Blodin; M. Leclerc; and G. Durocher, *J. Phys. Chem. B*, 104, **2000**, 9118-9125.

[24] A. A. Argun; P. H. Aubert; B. C. Thompson; I. Schwendeman; C. L. Gaupp; J. Hwang; N. J. Pinto; D. B. Tanner; A. G. MacDiarmid; and J. R. Reynolds, *Chem. Mater.,* 16, **2004**, 4401-4412.

[25] B. L. Dias; E. M. Girotto; R. de Matos; M. J. L. Santos; M. D. Paoli; and W. A. Gazotti, *J. Braz. Chem. Soc.,* 16, **2005**, 733-738.

[26] V. Hernandez; and J. T. L. Navarrete, *J. Chem. Phys*., 101, **1994**, 1369-1377.

[27] G. Shi; J. Xu; and M. Fu, *J. Phys. Chem. B*, 106, **2002**, 288-292.

[28] J. Cornil; D. A. dos Santos; D. Beljonne; and J. L. Bredas, *J. Phys. Chem.,* 99, **1995**, 5604-5611.

[29] M. J. Frisch; G. W. Trucks; H. B. Schlegel; G. E. Scuseria; M. A. Robb; J. R.Cheeseman; J. A. Montgomery; Jr. T. Vreven; K. N. Kudin; J. C. Burant; J. M. Millam; S. S. Iyengar; J. Tomasi; V. Barone; B. Mennucci; M. Cossi; G. Scalmani; N. Rega; G. A. Petersson; H. Nakatsuji; M. Hada; M. Ehara; K. Yota; R. Fukuda; J. Hasegawa; M. Ishida; T. Nakajima; Y. Honda; O. Kitao; H. Nakai; M. Klene; X. Li; J. E. Knox; H. P. Hratchian; J. B. Cross; C. Adamo; J. Jaramillo; R. Gomperts; R. E. Stratmann; O. Yazyev; A. J. Austin; R. Cammi; C. Pomelli; J.

W. Ochterski; P. Y. Ayala; K. Morokuma; G. A. Voth; P. Salvador; J. J. Dannenberg; V. G. Zakrzewski; S. Dapprich; A. D. Daniels; M. C. Strain; O. Farkas; D. K. Malick; A. D. Rabuck; K. Raghavachari; J. B. Foresman; J. V. Ortiz; Q. Cui; A. G. Baboul; S. Clifford; J. Cioslowski; B. B. Stefanov; G. Liu; A. Liashenko; P. Piskorz; I. Komaromi; R. L. Martin; D. J. Fox; T. Keith; M. A. Al-Laham; C. Y. Peng; A. Nanayakkara; M. Challacombe; P. M. W. Gill; B. Johnson; W. Chen; M. W. Wong; C. Gonzalez; and J. A. Pople, *Gaussian 03, Revision B.01*, Gaussian, Inc., Pittsburgh, PA, **2003**.

[30] M. Theander; O. Inganäs; W. Mammo; T. Olinga; S. Mattias; and M. R. Andersson, *J. Phys. Chem. B*, 103, **1999**, 7771-7780.

[31] E. Zhou; J. Hou; C. Yang; and Y. Li, *J. Polym. Scie. A: Polymerchem*., 44, **2006**, 2206-2214.

[32] G. Distefano; M. D. Colle; D. Jones; M. Zambianchi; L. Favaretto; and A. Modelli, *J. Phys. Chem.,* 97, **1993**, 3504-3509.

[33] S. Samdal; E. J. Samuelsen; and H. V. Volden, *Synth. Met*., 59, **1993**, 259-265.

[34] M. Graström; and O. Inganäs, *Synth. Met.,* 48, **1992**, 21-31.

[35] N. Dicesáre; M. Belletête; C. Marrano; M. Leclerc; and G. Durocher, *J. Phys. Chem. A*, 103, **1999**, 795-802.

[36] M. Rubio; M. Merchán; E. Orti; and B. O. Roos, *J. Chem. Phys.,* 102, **1995**, 3580-3586.

[37] N. Dicesére; M. Belletête; M. Leclerc; and G. Durocher, *J. Phys. Chem. A*, 103, **1999**, 803-811.

[38] J. L. Brédas; G. B. Street; B. Thémans; and J. M. André, *J. Chem. Phys.,* 83, **1985**, 1323-1329.

[39] D. Jones; M. Guerra; L. Favaretto; A. Modelli; M. Fabrizio; and G. Distefano, *J. Phys. Chem.,* 94, **1990**, 5761-5766.

[40] N. Dicésare; M. Belletête; C. Marrano; M. leclerc; and G. Durocher, *J. Phys. Chem. A*, 102, **1998**, 5142-5149.

[41] L. Cuff; and M. Kertesz, *J. Chem. Phys.,* 106, **1997**, 5541-5553.

[42] G. Zhang; Y. Pei; J. Ma; and C. L. Chen, *J. Phys. Chem. B*, 108, **2004**, 6988-6995.

[43] W. J. D. Beenken; and T. Pullerits, *J. Phys. Chem. B*, 108, **2004**, 6164-6169.

[44] A. C. Kolbert; N. S. Sariciftci; K. U. Gaudl; P. Bäuerle; and M. Mehring, *J. Am. Chem. Soc.,* 113, **1991**, 8243-8246.

[45] L. S. Roman; W. Mammo; L. A. A. Pettersson; M. R. Andersson; and O. Inganäs, *Adv. Mater.,* 10, **1998**, 774-777.

[46] A. C. Alguno; W. C. Chung; R. V. Bantaculo; R. M. Vequizo; H. Miyata; E. W. Ignacio; and A. M. Bacala, *NECTEC Tech. J.,* 9, **2001** ,215-218.

[47] U. Salzner; J. B. Lagowski; P. G. Pickup; and R. A. Poirier, *Synth. Met*., 96, **1998**, 177-189.

[48] A. K. Bhshi; and P. Rattan, *J. Chem. Soc., Faraday Trans*., 94, **1998**, 2823-2826.

[49] J. P. Ferraris; and T. L. Lambert, *J. Chem. Soc. Chem. Commun*., **1991**, 1268-1270.

[50] H. Subramanian; and J. B. Lagowski, *Int. J. Quant. Chem*., 66, **1998**, 229-240.

[51] M. Knupfer; D. Fichou; and J. Fink, *Phys. Rev. B,* 63, **2001**, 165203(1-4).

[52] F. C. Grozeman; L. P. Candeias; M. Swart; P. T. V. Duijnen; J. Wildeman; G. Hadziioanou; L. D. A. Siebbeles; and J. M. Warman, *J. Chem. Phys*., 117, **2002**, 11366-11378.

[53] G. Moro; G. Scalmani; U. Cosentino; and D. Pitea, *Synth. Met*., 108, **2000**, 165-172.